NT05

Large Scale Production, Selective Synthesis and Applications of Carbon NT by CCVD Process

Morinobu Endo

Shinshu University, Japan

Acknowledgements

Prof. M. S. Dresselhaus

Prof. H. W. Kroto

Madame A. Oberlin

Prof. D. Tomanek (MSU)

Profs. M. & H. Terrones (ICPyT)

Prof. R. Saito (Tohoku Univ.)

Prof. J. -C. Charier (UCL)

Profs. T. Hayashi and Y. A. Kim (Shinshu Univ.)

Outline

1. **CCVD process, historical aspect and present status**
2. **Mass production, current and near-future applications of CNTs**
3. ***Pathological Aspects* and Medical applications**
4. **DWNTs: heat treatment, Boron doping**
5. **Conclusions**

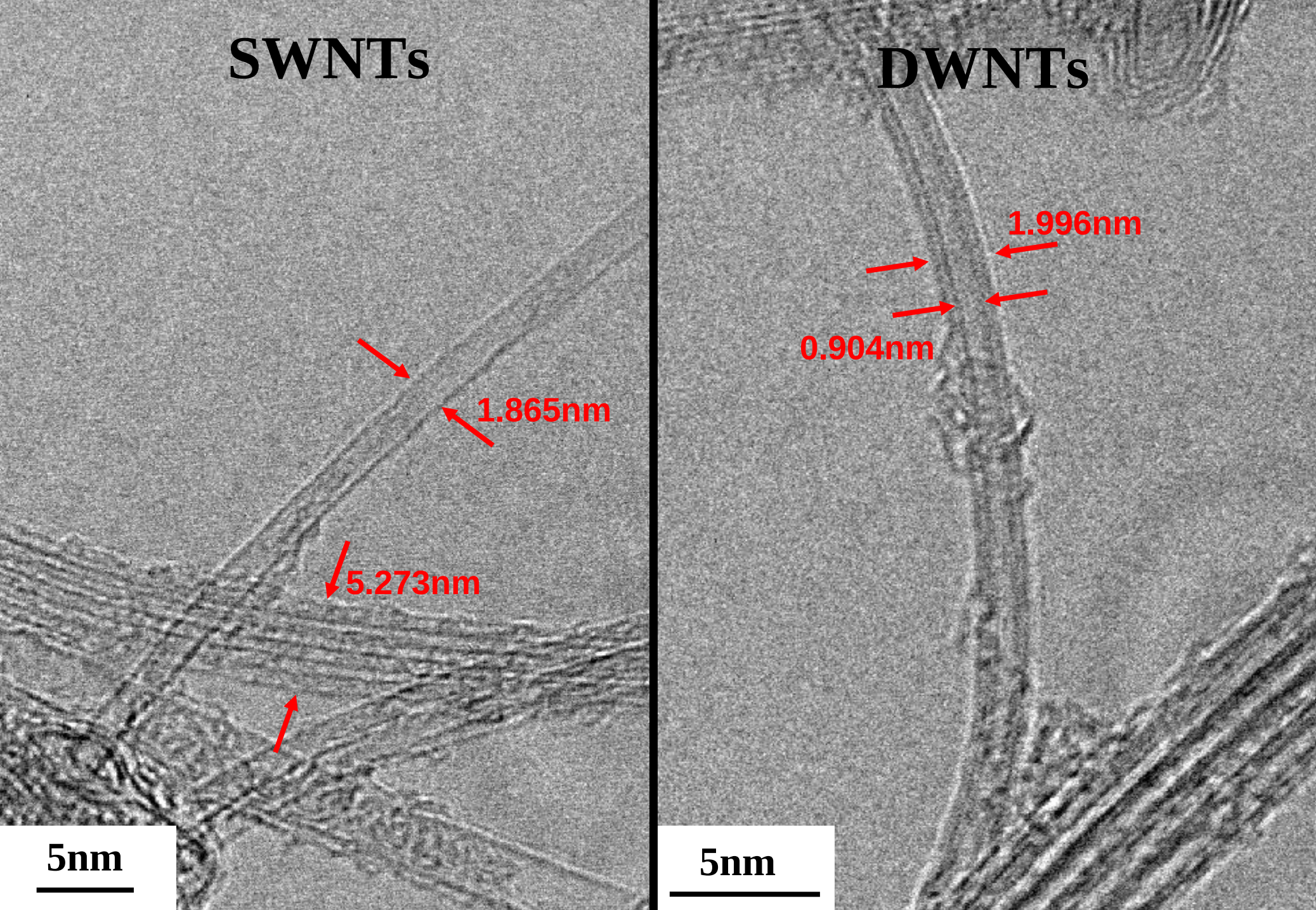
SWNTs
1.865nm
5.273nm
5nm
DWNTs
1.996nm
0.904nm
5nm

The structural controllability of CNT is the most important issue as a nanotech-material

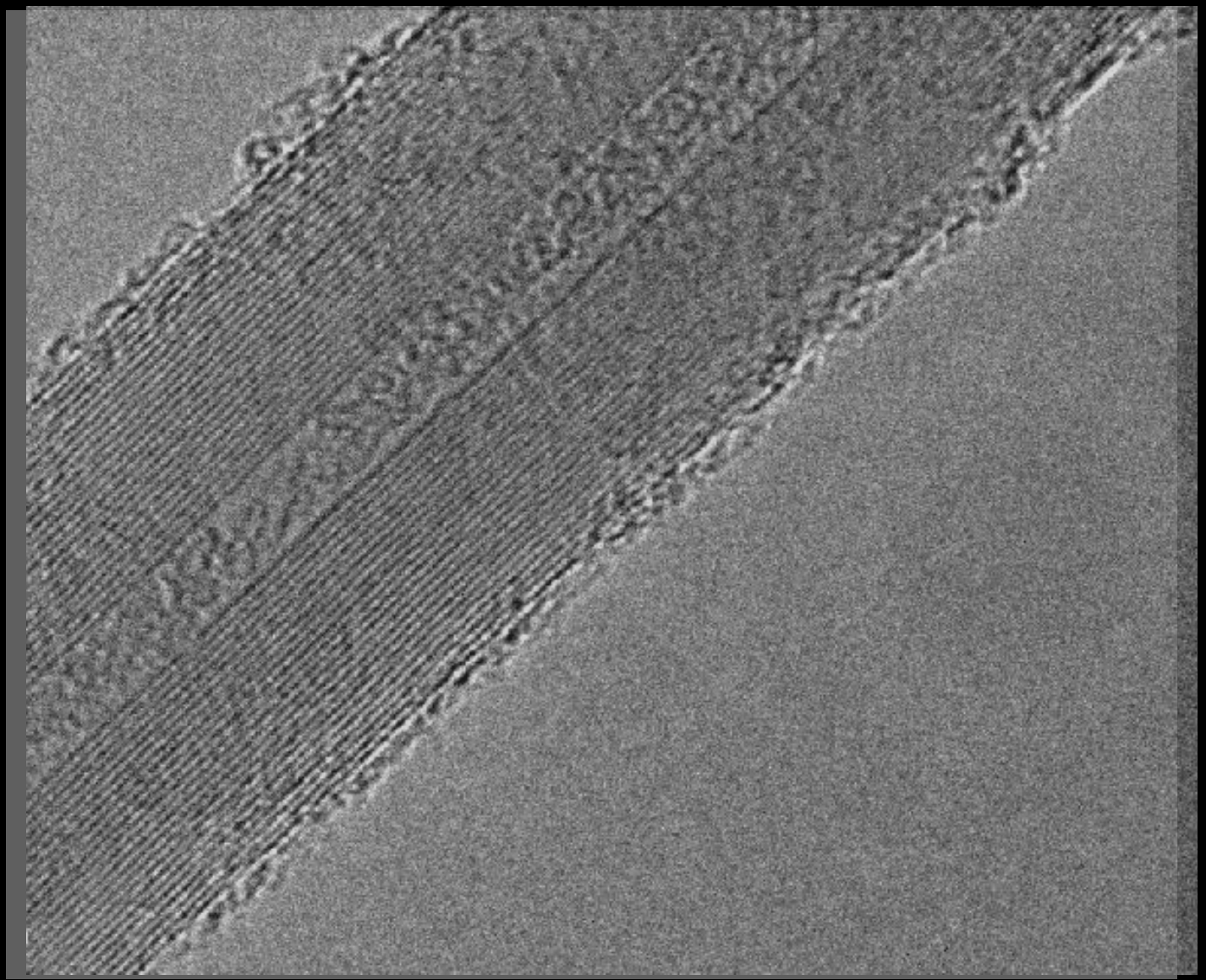

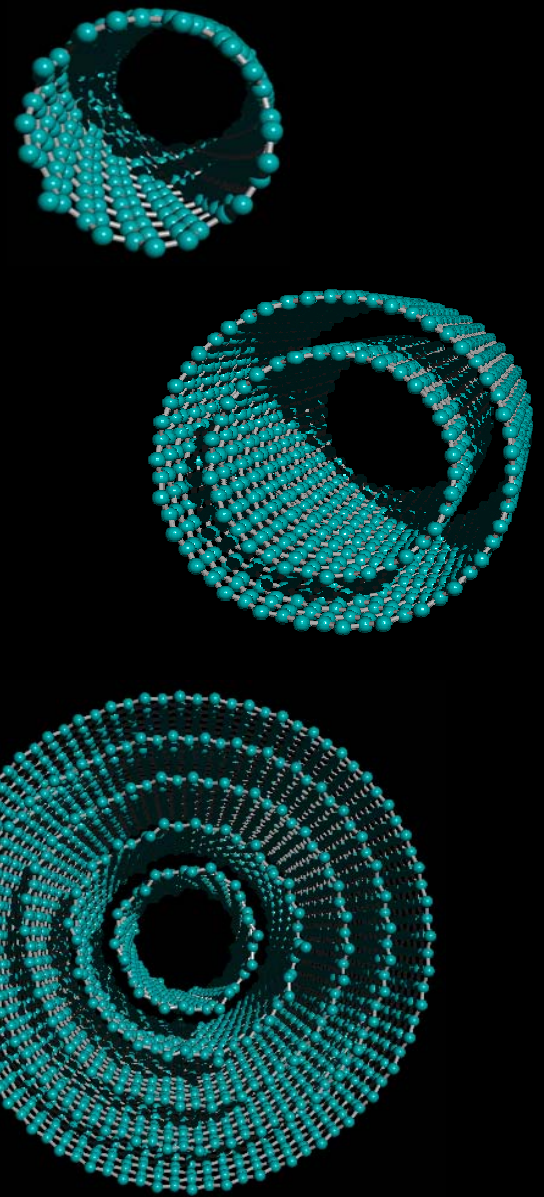


Cross-section
of VGCF
2μm

Manufacturing Apparatus for VGCFs

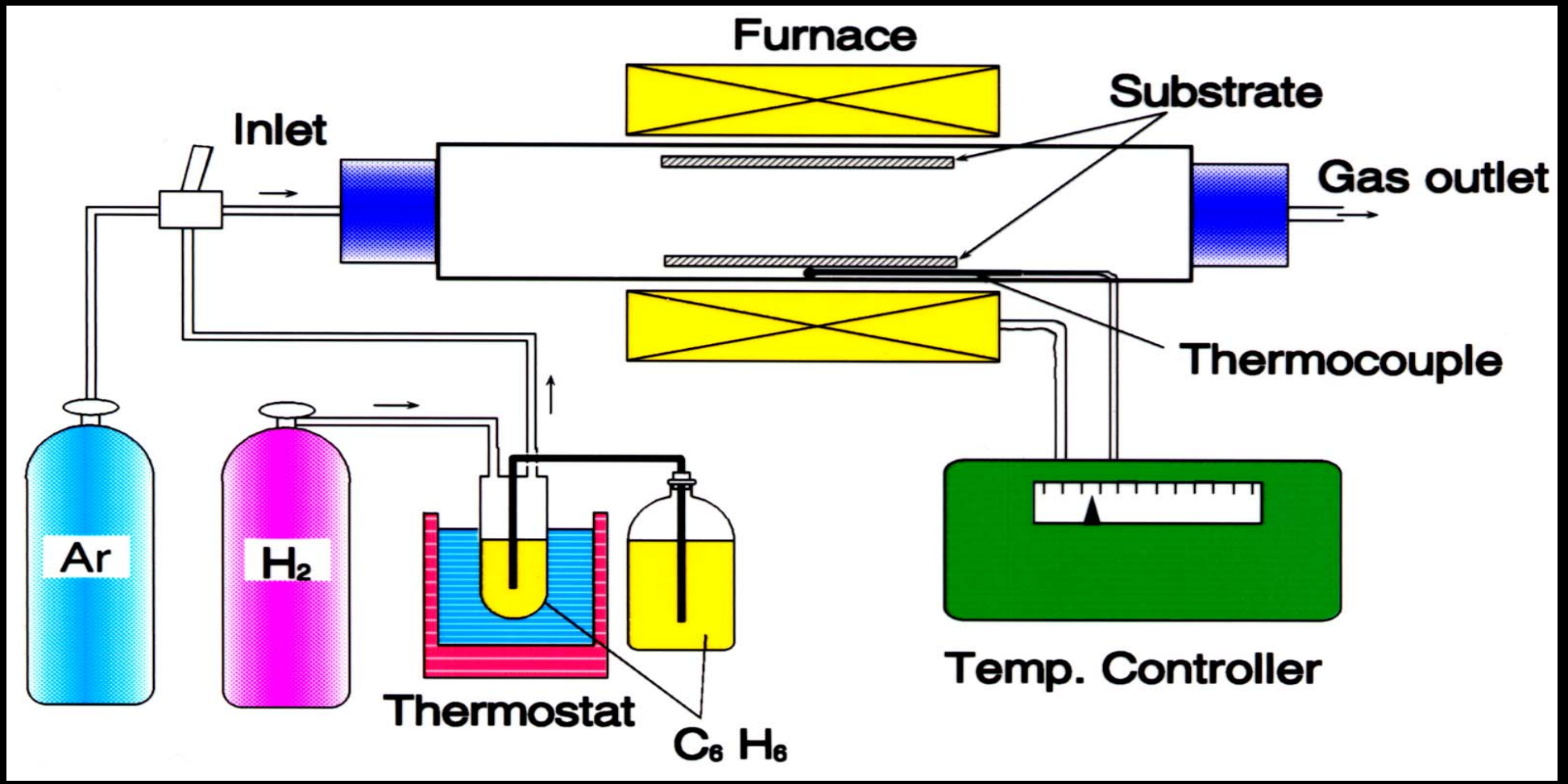

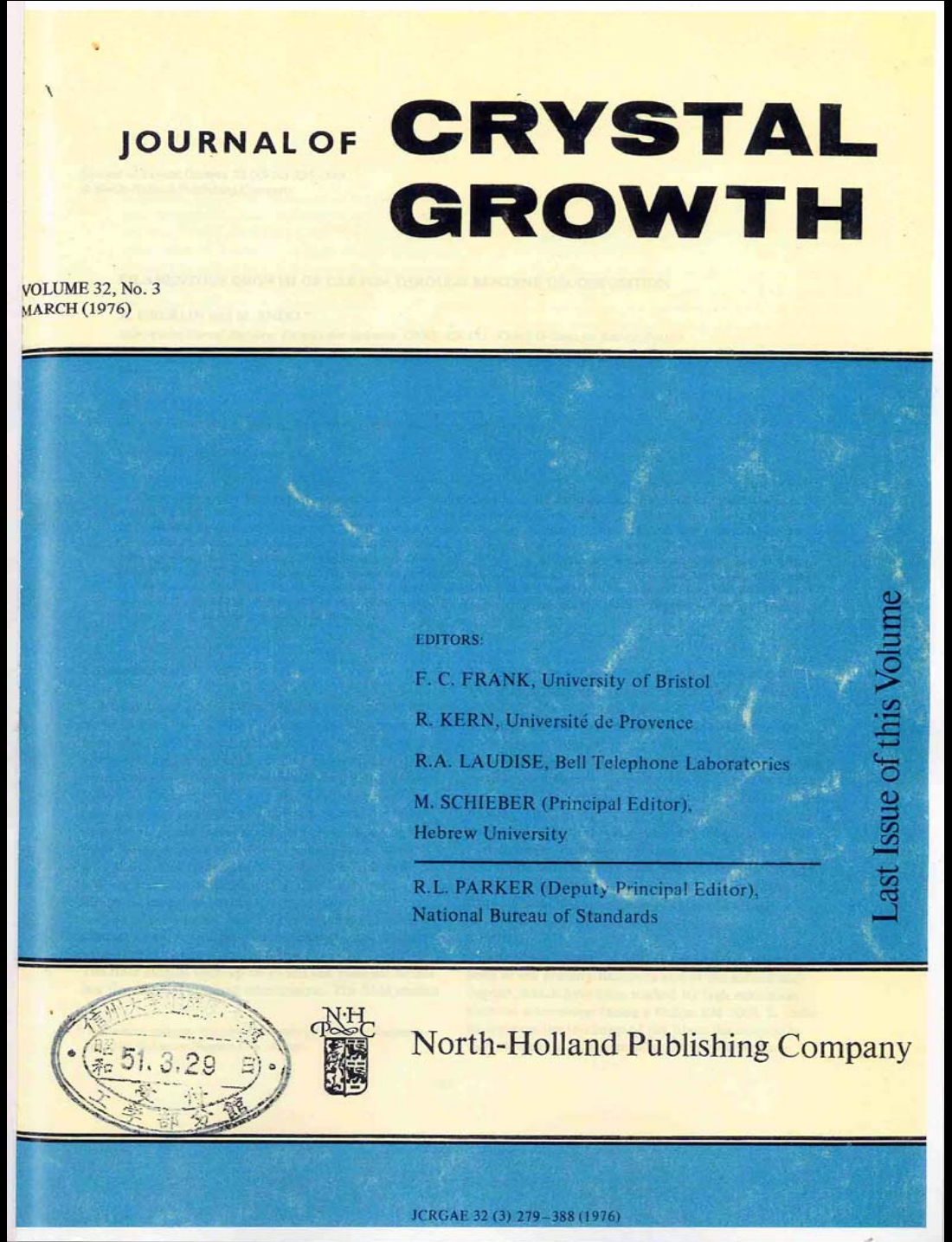

J. Cryst. Grow. 32
(1976) 335-349

A. Oberlin,
M. Endo,
and
A. T. Koyama

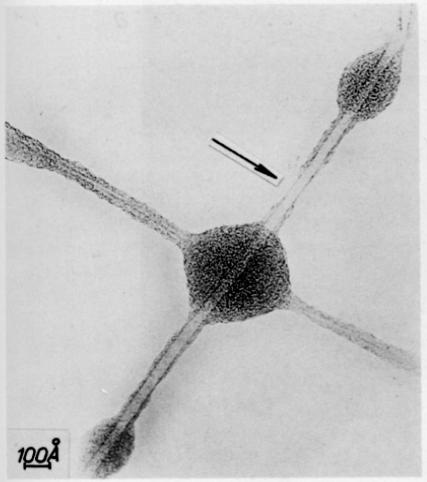

Fig. 11. Bright-field image of branched inhomogeneous fibres.

carbon atoms in a single carbon layer. Fig. 10c also shows that, near the hollow tube, the 00.2 fringes, i.e. the carbon layers, are very long, straight and perfectly parallel. The parallelism of the layers is so perfect in the vicinity of the tube that they always seem to form only one stack, thus explaining the 00.2 Bragg fringe production (which is not necessarily related to any three-dimensional order but only due to the perfect parallelism of the layers). The length of the fringes is usually more than 1000 Å. On the contrary, fig. 10d corresponding to the external part of the fibre only shows short fringes (less than 10 Å) piled up by two or three. The misorientation of one stack relatively to its neighbour ranges from 20 to 30°. This value satisfactorily agrees with the results deduced from SAD patterns. Sizes of the carbon layer stacks obtained from fringes are also in good agreement with those deduced from dark-field pictures.

The above results strongly support the occurrence of two growth processes. The first one is responsible for the formation of the inner core containing long, straight and parallel carbon layers cylindrically rolled around a hollow tube. The secondary process is the thickening of the fibre by a pyrolytic deposit. Some

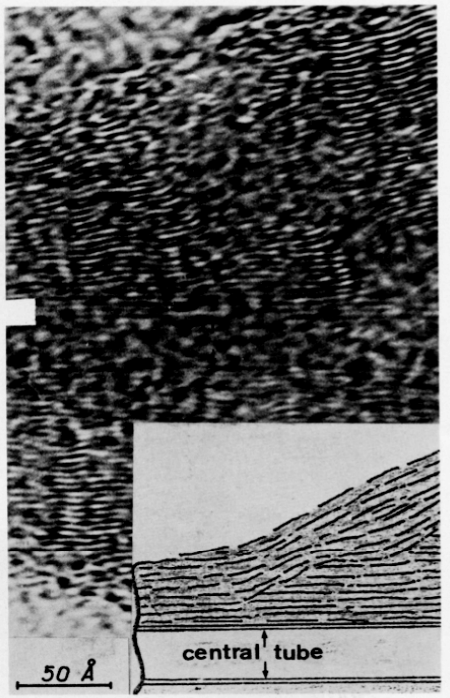

Fig. 12. (a) 00.2 lattice fringes of a constricted fibre, (b) schematic drawing of (a).

examples may be found where the internal core is only present in some part of a given fibre (see arrow in fig. 11). The same figure shows that some secondary deposit has been formed from place to place. This fact explains the conical shape of some fibres (see fig. 1c) which is probably due to an additional continuous pyrolytic deposit on an ancient one, similar to the one pictured in fig. 11. This mechanism is illustrated by lattice-imaging in the case of figs. 12a and 12b.

2.2. Tip of the fibres

Most of the fibre extremities are broken, but some of them are naturally terminated. In this latter case,

J. Cryst. Growth, 32 (197
335-349

Oberlin,
M. Endo,
and
T. Koyama

The first one is responsible for the formation of the inner core containing long, straight and parallel carbon lavers cylindrically rolled around a hollow tube.

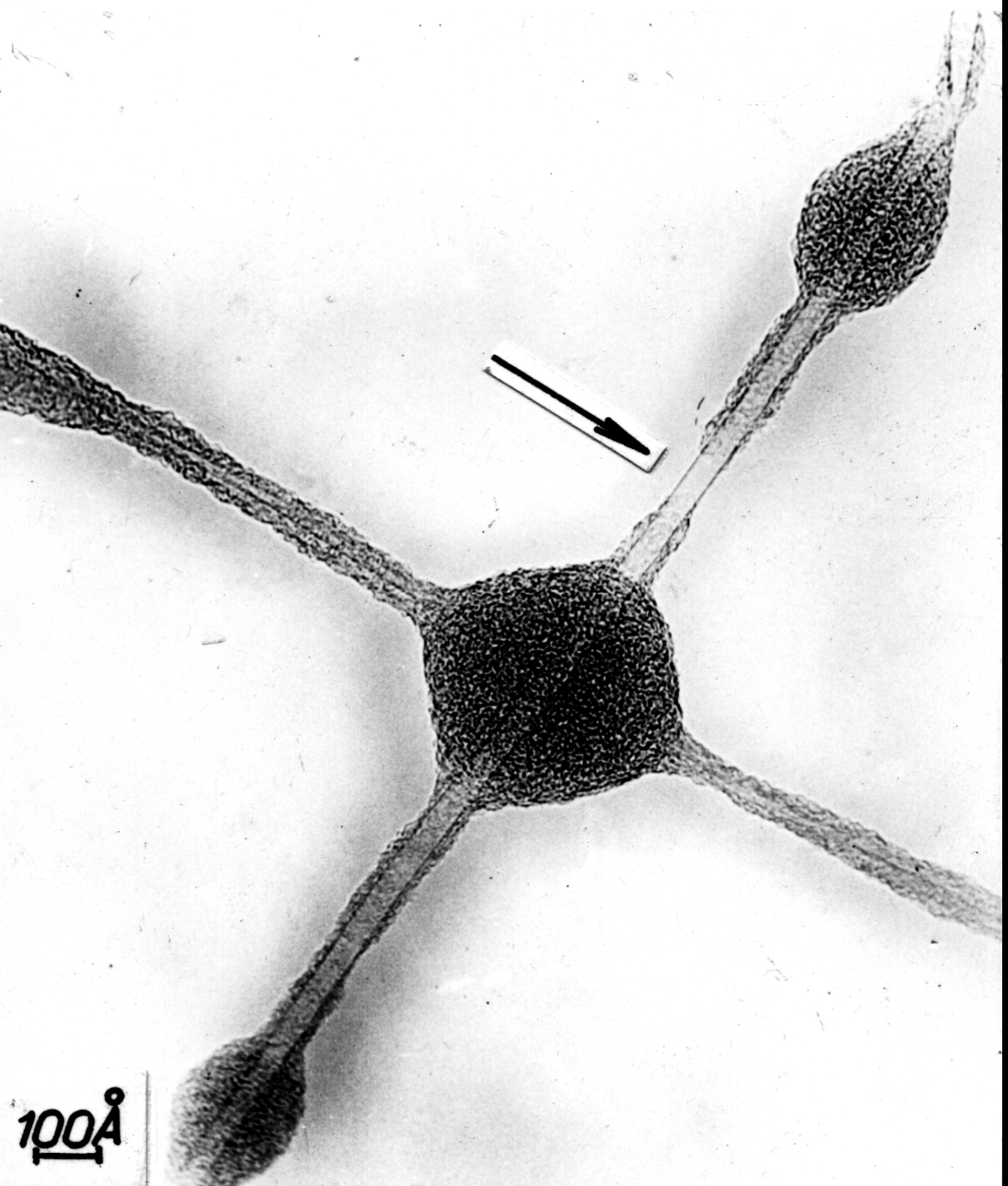

Exposed SWNT during the growth of crossing the tubes ;

J. Cryst. Growth, 32 (1976) 335-349、A.Oberlin, M. Endo,

and T. Koyama

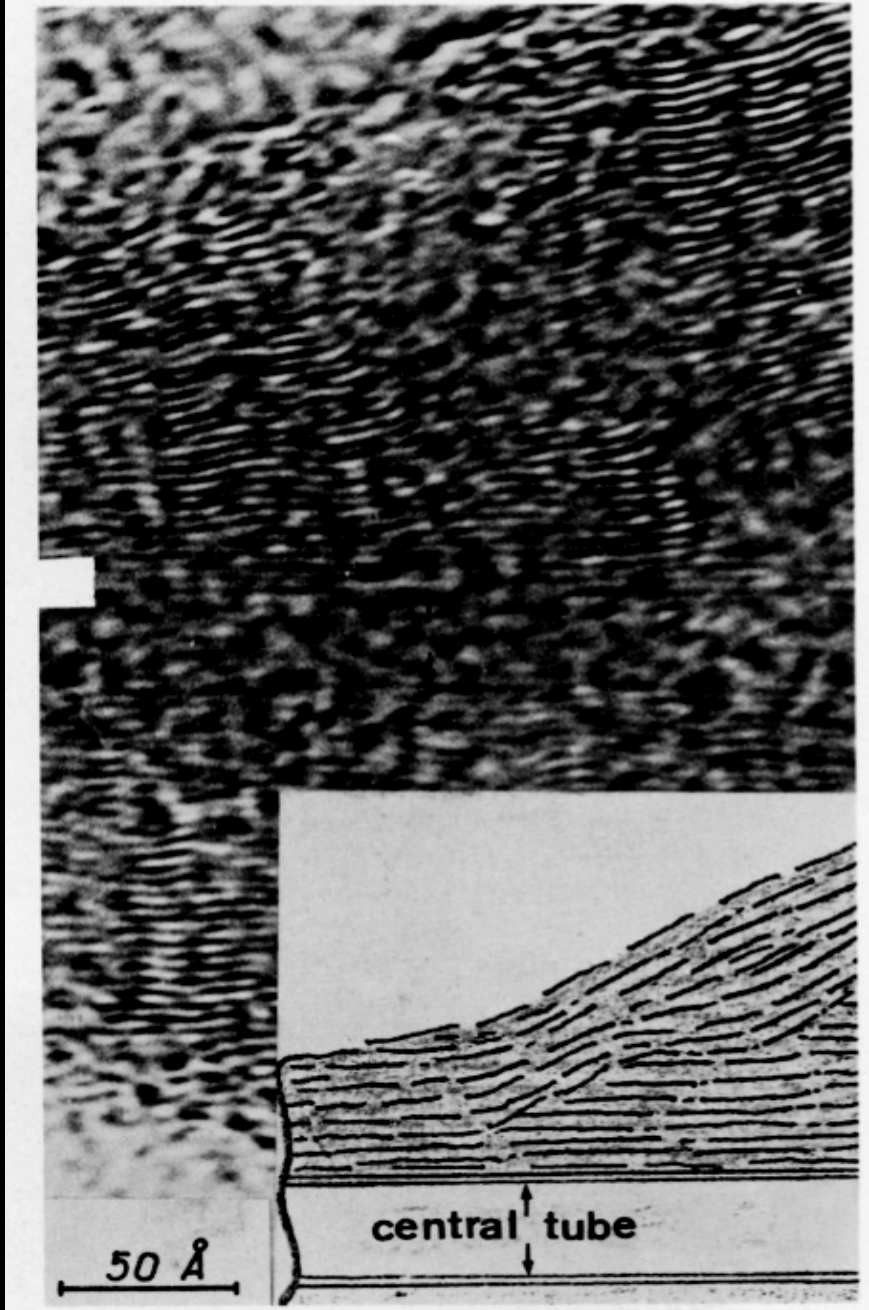

Fig. 12. (a) 00.2 lattice fringes of a constricted fibre, (b) schematic drawing of (a).

J. Cryst. Grow. 32 (1976)
335-349
A. Oberlin, M. Endo,
and T. Koyama

Double layered carbon nanotube in the core of the VGCF

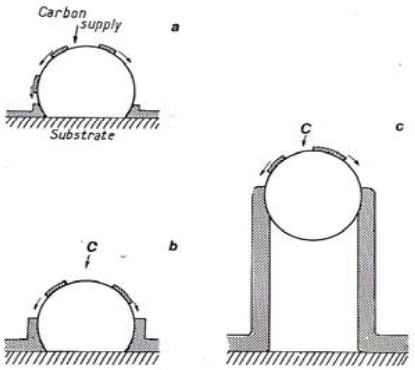

Fig. 21. Schematic illustration of fibre growth through catalytic effect.

the droplet. The carbon thus tends to nucleate on the side portions of the drop unprotected from carbon deposition because of their contact with the furnace. All these interpretations consider the diffusion of carbon atoms either through the metal or through the carbide and do not take into account any possible diffusion of metal into carbon. Moreover all of them do not really satisfactorily explain anisotropy of the growth and the occurrence of a central hollow tube.

An explanation which seems more satisfactory has been proposed by Baird et al. [26] involving a surface diffusion of "metal–metal hydrocarbon species" across the edge of the carbon layer planes. At the beginning small "liquid-like" droplets of iron get fixed on the wall of the furnace, resulting from the reduction by hydrogen of iron oxide soots. On that clean surface begins to nucleate an association of metal and hydrocarbons which diffuses on the surface and dissociates at the contact angle between the droplet and the wall of the furnace acting as a substrate. The beginning of a carbon shell is then produced. New metal hydrocarbon species dissociate on its edges and the carbon layers develop by lateral growth following the external surface of the catalyst (figs. 21a and 21b). Such a lateral growth exerts a force strong enough to lift up the catalyst particle above the surface of the substrate (fig. 21c). Layers always progress laterally in the same way and result in a filament. The hollow channel in the centre is due to the fact that no carbon supply can reach the back of the droplet, the surface of which is protected from downward surface migration by the lateral carbon layers. Growth of carbon layers would continue as long as there is a supply of metal from the top of the catalyst particle (the metal being progressively trapped between the carbon layers). When the whole droplet is covered by carbon layers at the tip, the diffusion stops and growth ends. This kind of mechanism is strongly supported by the existing relics of cementite found inside the carbon shell (see fig. 20). It must be noticed that cementite crystals are obviously formed only when cooling occurs. Such a mechanism also well explains branching of the fibres.

Increase in thickness by pyrolytic deposit on the primary thin fibres is a common phenomenon leading to graphitizable carbon. The constricted aspects often encountered at that stage of growth are probably due to the temperature gradient created along the fibre axis by a catalyst particle existing in that place. This may also be due to fluctuations of the gas flow in the reaction furnace. Anyway, such a deposit is similar to pyrolytic carbon, i.e. it is strongly oriented with its carbon layers approximately parallel to the substrate; but it is made of small turbostratic stacks with tilt and twist boundaries and thus looks more defective than the catalytic carbon contained in the core.

References

[1] W.R. Davis, R.J. Slawson and C.R. Rigby, Nature 171 (1953) 756.
[2] L.J.E. Hoffer, E. Stering and J.T. MacCartney, J. Phys. Chem. 59 (1955) 1153.
[3] L. Meyer, Z. Krist. 109 (1957) 61.
[4] M. Hillert and N. Lange, Z. Krist. 111 (1958) 24.
[5] R. Bacon, J. Appl. Phys. 31 (1960) 283.
[6] M.L. Lieberman, C.H. Hills and C.J. Miglionico, Carbon 9 (1971) 633.
[7] F.E. Wawner, Jr., J. Appl. Phys. 44 (1973) 502.
[8] T. Koyama, M. Endo and Y. Onuma, Japan. J. Appl. Phys. 11 (1972) 445.
[9] T. Koyama and M. Endo, Oyo Buturi 42 (1973) 690.
[10] T. Koyama and M. Endo, Japan. J. Appl. Phys. 13 (1974) 1175.
[11] T. Koyama, M. Endo and Y. Hishiyama, Japan. J. Appl. Phys. 13 (1974) 1933.
[12] A. Oberlin and G. Terrière, J. Microscopie 14 (1972) 1.

J. Cryst. Grow. 32
(1976) 335-349

A. Oberlin,
M. Endo,
and
A. T. Koyama

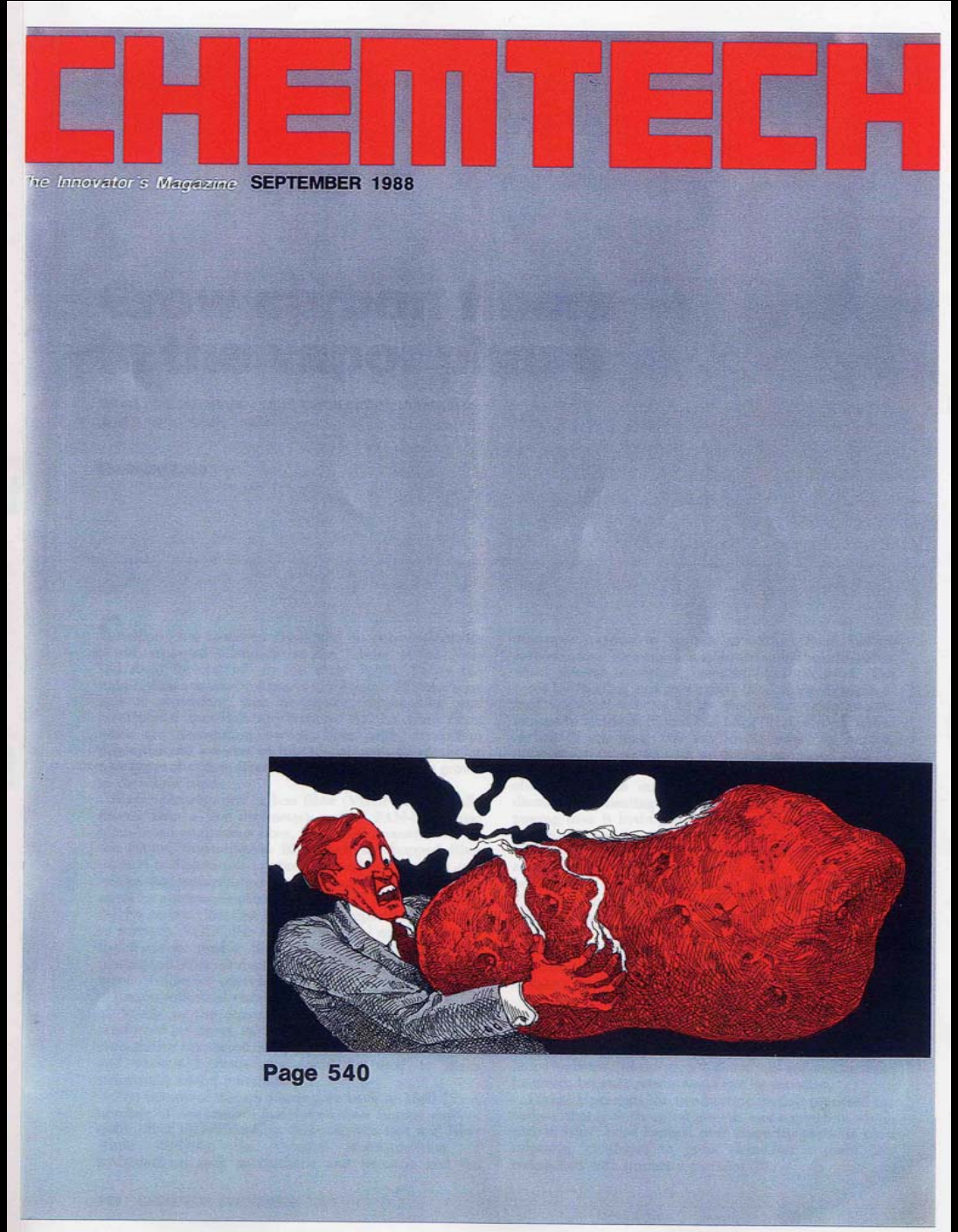

M. Endo

American Chemical Society,

CHEMTECH, September, pp.568-576, (1988).

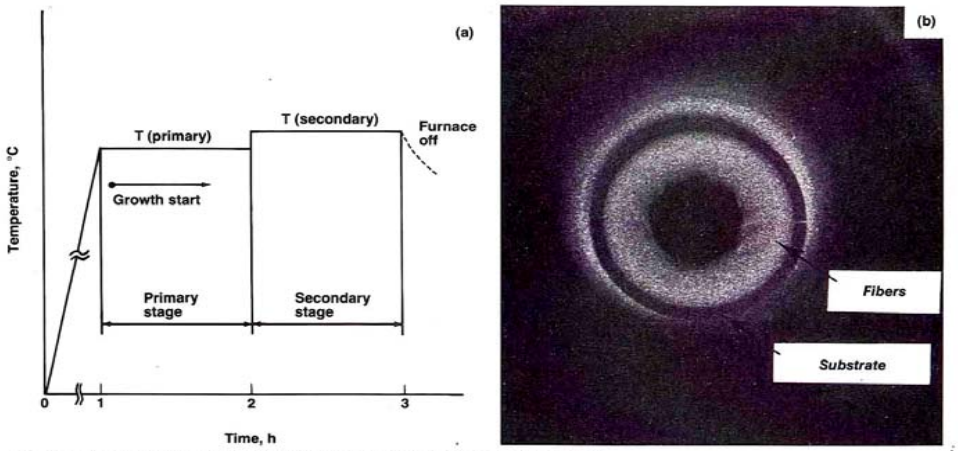

Figure 3. Temperature program (a); fiber growing in the furnace at 1100 °C (b)

Figure 2 depicts VGCF production equipment. A mixture of hydrogen and hydrocarbon is admitted into a reaction tube in an electrical furnace and kept around 1100 °C. Carbon fiber forms over a substrate in the reaction tube.

VGCF thus formed is grown in two steps: the fiber first forms over fine catalyst particles of iron or other relevant metals dispersed over the substrate; it then grows in the radial direction, resulting in fibers several decimeters long and about 10 μm in diameter. Temperature and timing are controlled throughout the process. Figure 3 shows temperature profiles and the fibers growing in the furnace. Note that VGCF is produced by a relatively simple system.

A scanning electron microscope (SEM) photograph of the fiber cross-section reveals a unique structure in which layers like growth rings lie concentrically on top of each other (Figure 4). VGCF has a circular cross-section and a preferred orientation in which networks of carbon planes are placed parallel to one another along the direction of the fiber axis. The orientational alignment is greater than those of conventional carbon fibers prepared in the same temperature range, which might account for the higher electrical conductivity and modulus of elasticity of VGCF.

One of the distinguishing structural features of VGCF is the presence of a hollow tube, about 10 nm or less in diameter, along the fiber axis (Figure 5a). The tube wall is composed of linearly extended, single-crystalline-like carbon layers, as shown in Figure 5c. Each layer, however, has a turbostratic stacking structure (i.e., is not a three-dimensional crystal) and does not form a three-dimensional graphite structure. The fiber periphery, on the other hand, is microcrystalline, in which two or three carbon basal networks are layered. This structure is common with thermally decomposed carbon films (Figure 5b). Thus it is apparent that the VGCF is composed of two different structures formed by different mechanisms: the catalytic growth of the fine, precursor fiber consisting of the hollow tube and linearly extended, parallel carbon layer faces near the fiber core; and the subsequent thermal decomposition of the hydrocarbons introduced by chemical vapor deposition that allows the fiber to grow in the radial direction. The physical properties of the resultant fibers are largely determined by the structures of the exterior region in thermal decomposition of hydrocarbons.

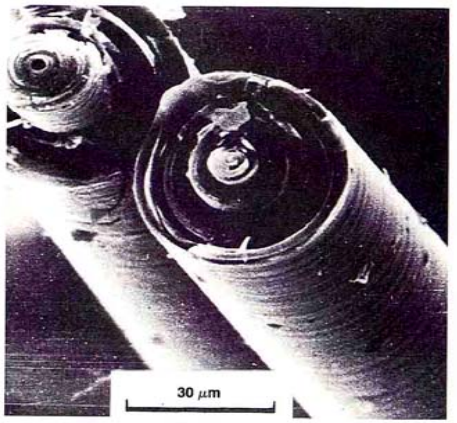

Figure 4. SEM image of VGCF cross-section

Mass production

The VGCF production process consists of three steps:

- seeding, in which ultrafine metallic catalyst particles serving as nuclei for the fiber growth are dispersed over the substrate surface,

M. Endo

American Chemical Society,

CHEMTECH, September, pp.568-576, (1988).

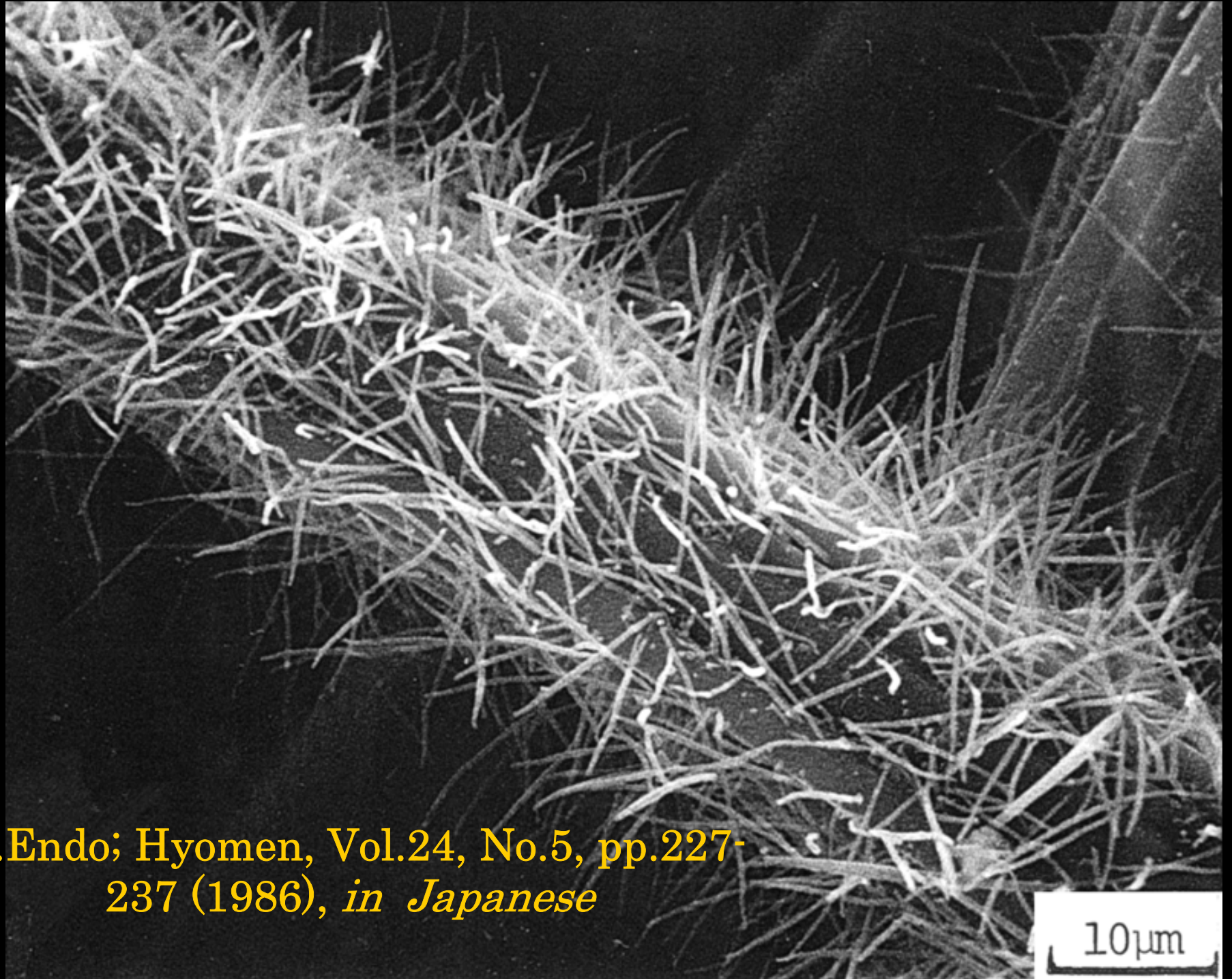

M.Endo; Hyomen, Vol.24, No.5, pp.227-237 (1986), *in Japanese*

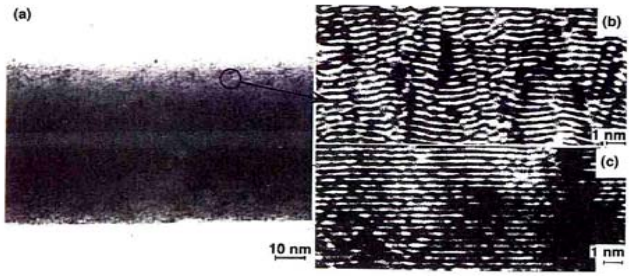

Figure 5. Hollow tube (a) and two different structures (b, c)

Figure 6. Substrate seeding methods

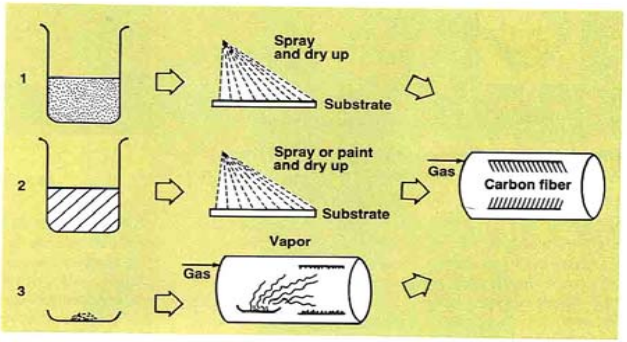

- growth of fine precursor fiber, and
- deposition of the thermally decomposed hydrocarbons over the precursor fiber to increase its radial size.

The dispersion of the fine catalyst particles, such as those of iron, is the key process for the mass production of VGCF. The seeding step largely determines the density of the growing fiber, i.e., the number of fibers per unit area of the substrate, and hence the productivity (7).

Figure 6 shows the three seeding approaches currently available. Approach 1 involves preparation of superfine particles of iron or other metals of 50 nm or less in size by an appropriate method such as evaporation in inert gas; the iron particles are suspended in alcohol to be sprayed and dried over a substrate. Particles having a magnetically or chemically active surface must be independently dispersed to achieve a dense growth of the fibers. Use of surfactants can promote uniform dispersion. Approach 2 attempts to spray a solution of a metal compound, such as iron nitrate, over a substrate; when heated to about 1100 °C in an electric furnace, ultrafine metal particles form. Approach 3 represents the direct seeding, in which ferrocene or other organic, metal-containing compounds are thermally decomposed and deposited over a substrate. This approach allows integration of the seeding with the subsequent fiber formation processes (9).

The seeded substrate is then heated in an electric furnace and a hydrogen–hydrocarbon mixture is passed over the substrate in a programmed process (Figure 3) to form VGCF (10 μm in diameter, 50–60 mm long). The density of the fiber formed in this manner will be about 600–1200 fibers/mm².

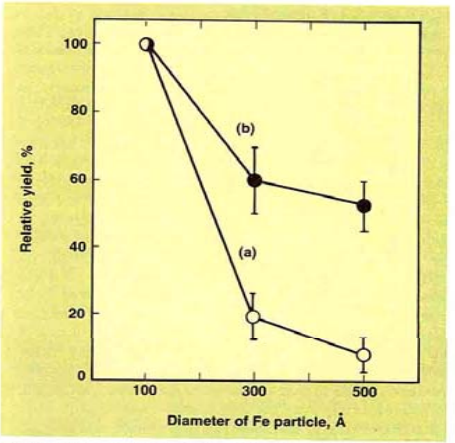

Figure 7. Effects of catalyst particle size on VGCF yield; catalyst with narrow (a) and broad (b) size distribution

Fiber yield increases with smaller catalyst particle size (Figure 7). Growth rate of VGCF in the axial direction is 1–50 mm/min, which is 3–4 orders of magnitude higher

M. Endo

American Chemical Society,

CHEMTECH, September, pp.568-576, (1988).

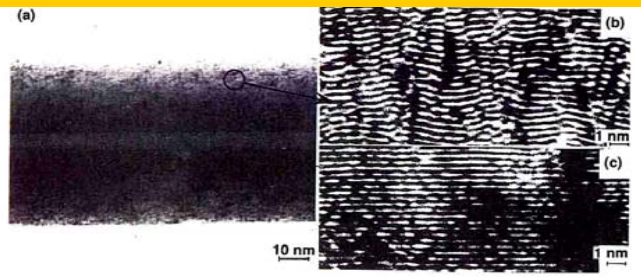

Figure 5. Hollow tube (a) and two different structures (b, c)

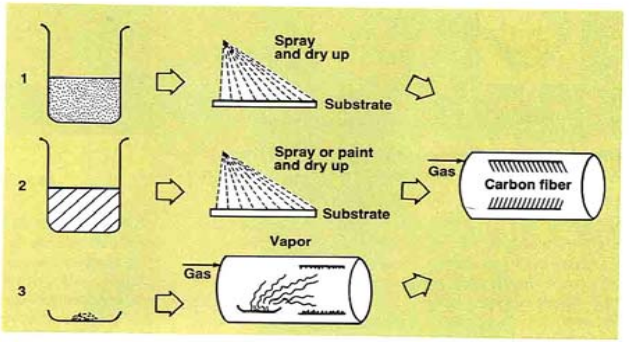

Figure 6. Substrate seeding methods

- growth of fine precursor fiber, and
- deposition of the thermally decomposed hydrocarbons over the precursor fiber to increase its radial size.

The dispersion of the fine catalyst particles, such as those of iron, is the key process for the mass production of VGCF. The seeding step largely determines the density of the growing fiber, i.e., the number of fibers per unit area of the substrate, and hence the productivity (7).

Figure 6 shows the three seeding approaches currently available. Approach 1 involves preparation of superfine particles of iron or other metals of 50 nm or less in size by an appropriate method such as evaporation in inert gas; the iron particles are suspended in alcohol to be sprayed and dried over a substrate. Particles having a magnetically or chemically active surface must be independently dispersed to achieve a dense growth of the fibers. Use of surfactants can promote uniform dispersion. Approach 2 attempts to spray a solution of a metal compound, such as iron nitrate, over a substrate; when heated to about 1100 °C in an electric furnace, ultrafine metal particles form. Approach 3 represents the direct seeding, in which ferrocene or other organic, metal-containing compounds are thermally decomposed and deposited over a substrate. This approach allows integration of the seeding with the subsequent fiber formation processes (9).

The seeded substrate is then heated in an electric furnace and a hydrogen–hydrocarbon mixture is passed over the substrate in a programmed process (Figure 3) to form VGCF (10 μm in diameter, 50–60 mm long). The density of the fiber formed in this manner will be about

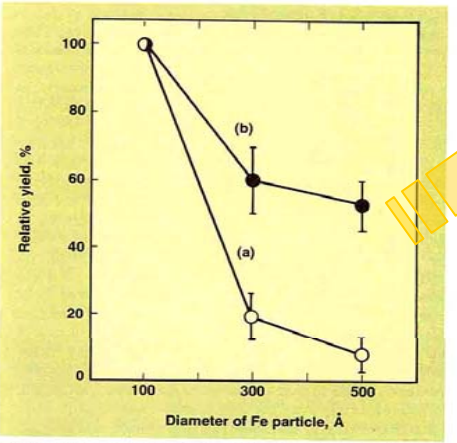

Figure 7. Effects of catalyst particle size on VGCF yield; catalyst with narrow (a) and broad (b) size distribution

600–1200 fibers/mm².

Fiber yield increases with smaller catalyst particle size (Figure 7). Growth rate of VGCF in the axial direction is 1–50 mm/min, which is 3–4 orders of magnitude higher

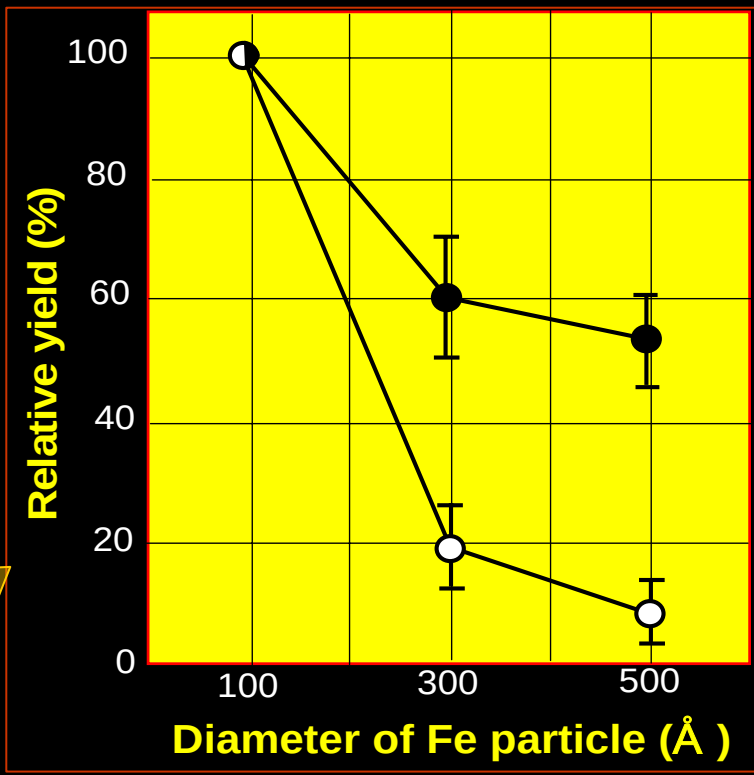

Fiber yield increases with smaller catalyst particle size (Figure 7). Growth rate of VGCF in the axial direction is 1–50 mm/min, which is 3–4 orders of magnitude higher

M. Endo American Chemical Society, CHEMTECH, September, pp.568-576, (1988).

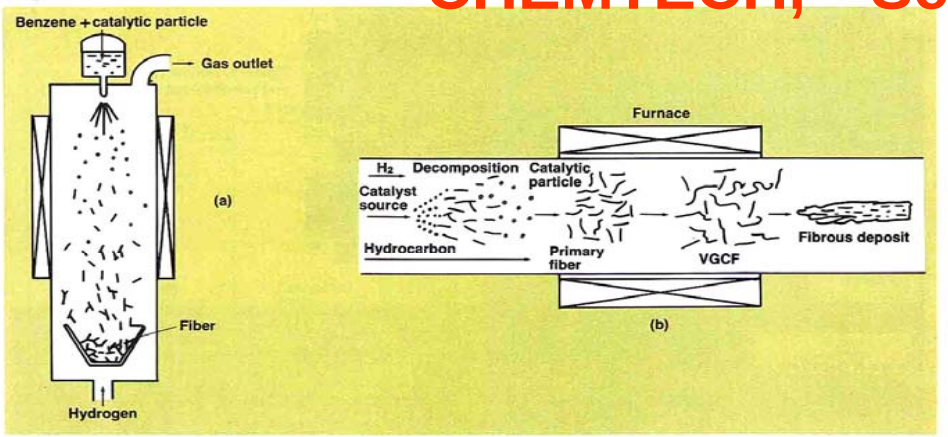

Figure 8. **Conceptual scheme of VGCF production over fluidizing catalyst particles by direct (a) and indirect (b) methods**

than those of conventional metallic or nonmetallic crystalline whiskers. This is largely due to the actions of the superfine catalyst particles.

We have developed fluidization seeding in which the initial fibers are formed over fluidized catalyst particles (Figure 8). It is much more efficient than substrate seeding for fiber formation (*9*).

Growth model and mechanism

As mentioned earlier, VGCF grows much faster than conventional whiskers, which grow at about 50 μm/s. VGCF having an aspect ratio (length/diameter) of 100 can be produced in several seconds. This ratio is equivalent to that of commercial whiskers like SiC. A reaction time of several seconds is sufficient for fine fibers to grow in a hydrocarbon atmosphere with virus-size or smaller catalyst particles. In the fluidization seeding process, the catalyst may be introduced into the reactor either directly or indirectly (Figure 8). The indirect method, by which the catalyst particles and VGCF form simultaneously, is based on Approach 3 (Figure 6). It can efficiently produce fine particles of several tens of angstroms, which, by fluidizing ultrafine metal particles introduced into the reactor in a controlled manner, greatly promotes fiber growth in the three-dimensional space of the reaction chamber. Fluidization seeding permits better control of the catalyst-feed ratio and the product aspect ratio. Fluidization-produced VGCF has a crystallographic structure similar to that of substrate-produced VGCF, but with much smaller hollow tubes of 2–3 nm (Figure 9).

It is interesting to note that the fluidization method can produce carbon fibers ranging from carbon black-like fibers with an aspect ratio of about 1 to ordinary continuous fibers, in which the aspect ratio is essentially infinite. Products having low aspect ratios can be used as reinforcing agents for various matrices, such as rubber, plastics, and cement.

Figure 10 shows the tip of a growing fiber with a crystal of iron carbide at the end of the hollow tube. The iron particle—which is either deposited on the substrate or fluidized—remains as it is while the fiber is growing but might react with the cementite particles when cooled. High-resolution transmission electron microscopy (TEM) has revealed that catalyst particles found at the fiber ends have fairly uniform sizes, mostly below 20–30 nm. Many fluidization-seeded particles are around 5 nm, which agrees with the observation that the fiber forms more efficiently with decreasing particle size. Baker and co-workers have reported that a finer particle grows the filamentous carbon faster (*10*), which may support our results for the ultrafine catalyst particles.

The fiber will continuously grow as long as the particles dispersed on the substrate or the fluidizing catalyst particles are active; the fiber ceases to grow when the particle surfaces are covered with carbon layers, oxygen, or other impurities, thus retarding the development of the carbon species. It is therefore vital to control the hydrocarbon partial pressure in the system and to keep the atmosphere free of impurities such as moisture and oxygen, in order to obtain long fibers. The TEM image (Figure 11) shows the catalyst particle at the end of the growing precursor fiber; it is not yet covered with hard, graphite-like carbon layers and can still actively assist fiber growth in the longitudinal direction. The resultant thin fibers have a continuous, thin, hollow tube as shown in Figure 11b.

We can illustrate the formation of VGCF by the model shown in Figure 12 (*11*). A reducing atmosphere of hydrogen at ~1100 °C reduces the catalyst particle of a transition metal such as iron, or cleans its surface, which promotes the polymerization and condensation of the hydrocarbon to develop hexagonal planar networks of carbon. They grow perpendicular to the substrate surface in the space between the particle and the substrate. The particle is driven upward, away from the substrate—presumably by osmotic pressure, surface tension, or

The TEM image shows the catalyst particle at the end of the growing precursor fiber; it is not yet covered with hard, graphite-like carbon layers and can still actively assist fiber growth in the longitudinal direction. The resultant thin fibers have a continuous, thin, hollow tube as shown in Figure 11b.

The Floating Seeding Method (Vertical type)

M. Endo; American Chemical Society, CHEMTECH, September, pp.568-576, (1988).

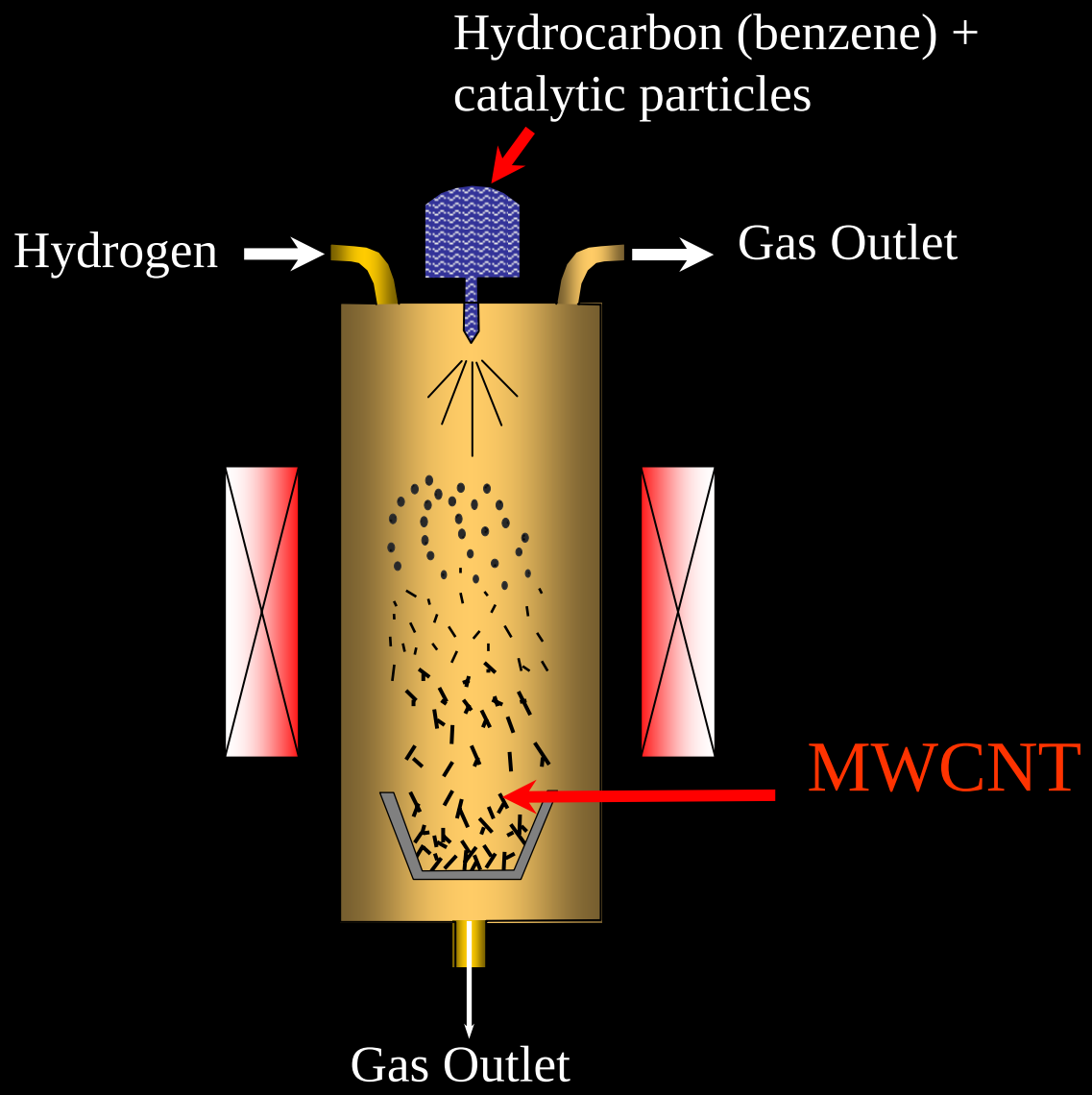

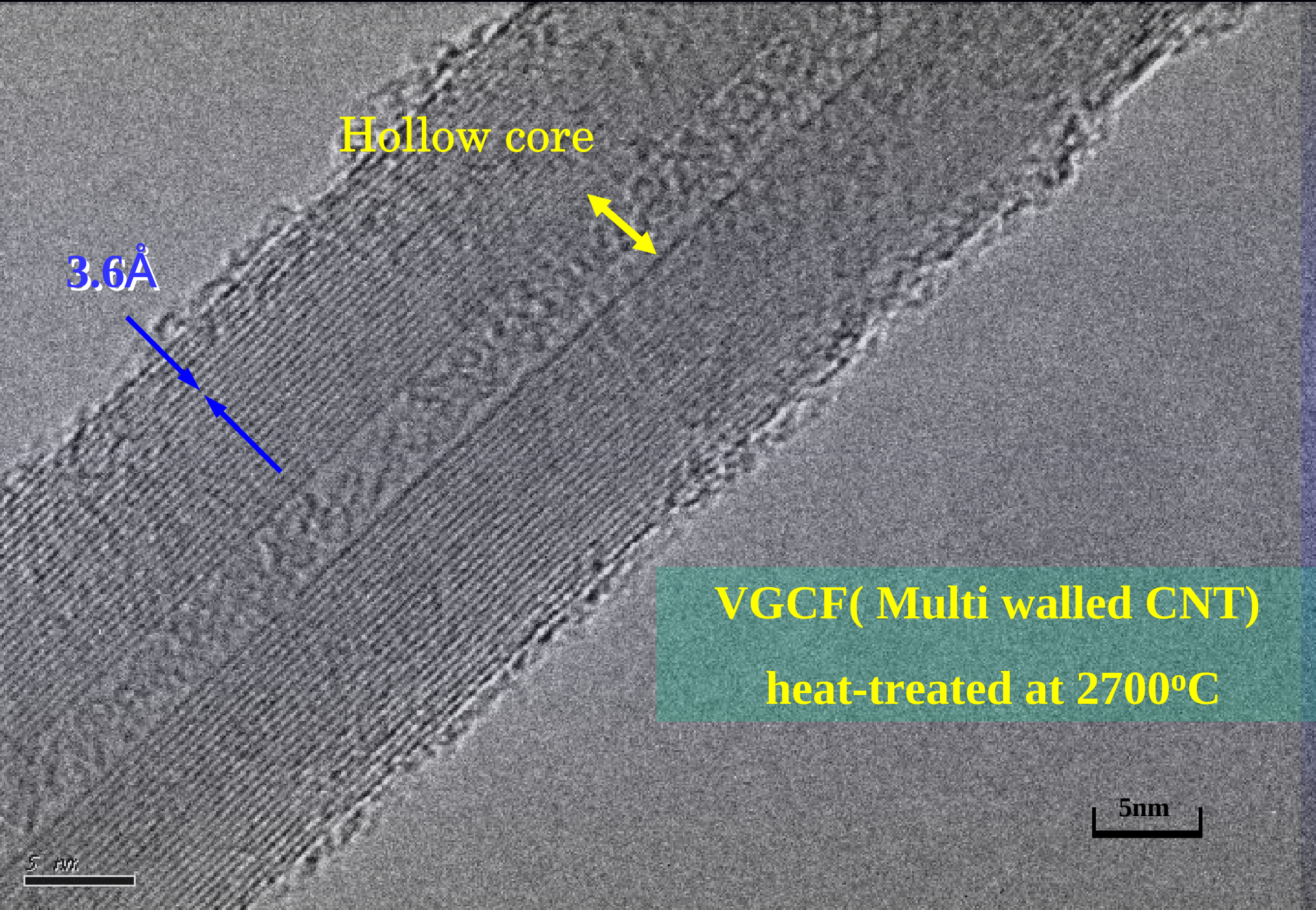
Hollow core
3.6Å
VGCF(Multi walled CNT)
heat-treated at 2700°C
5nm
5 nm

Structure of LIB practical cell

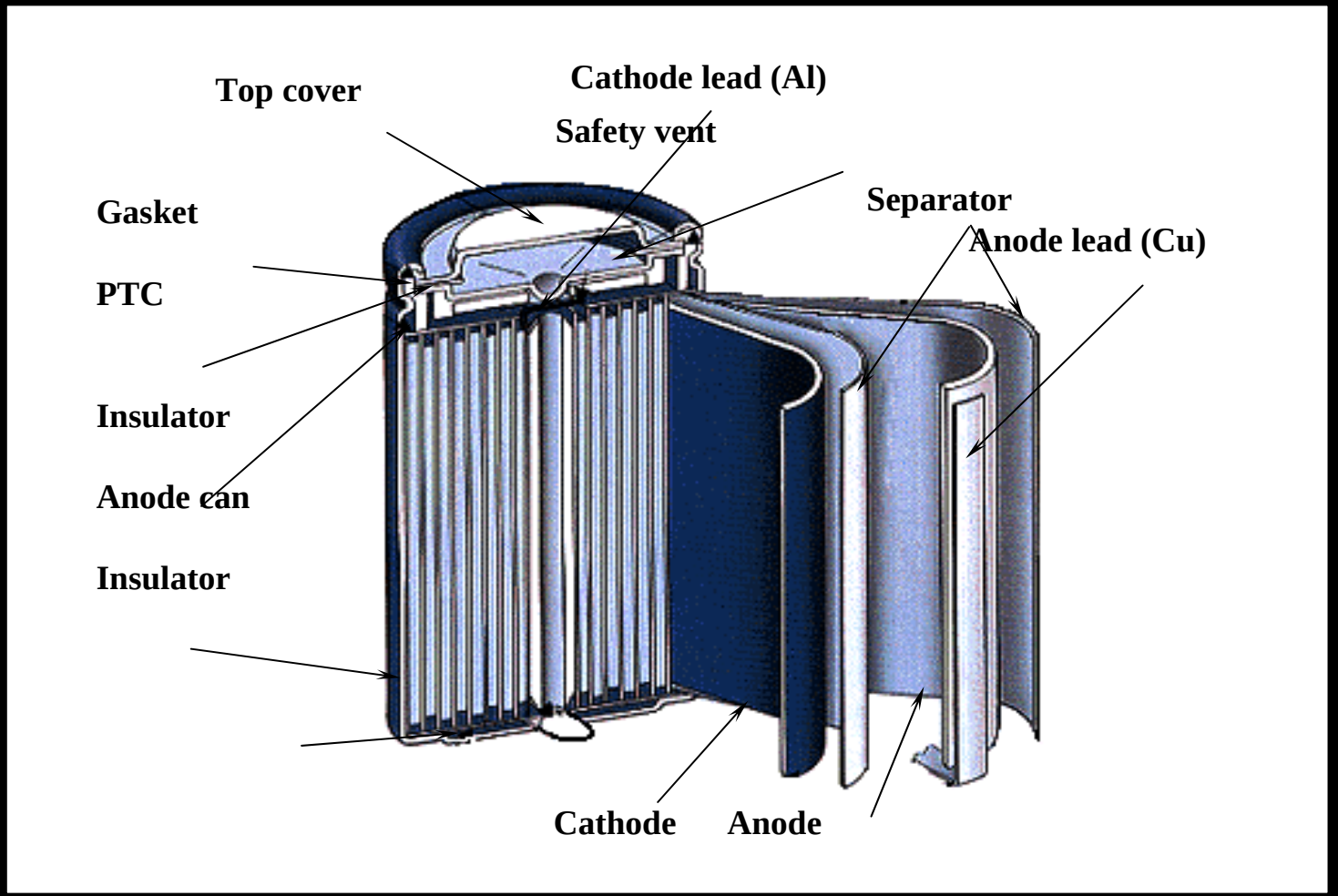

Ref : Sony's catalog, Lithium ion rechargeable battery, ACG-4012-N-9707-P3-002, 1977.
M. Endo, T. Karaki, T. Fujino New ceramics 1988; 4: 46-52, (In Japanese)

Principle of operation of Li-ion-Battery

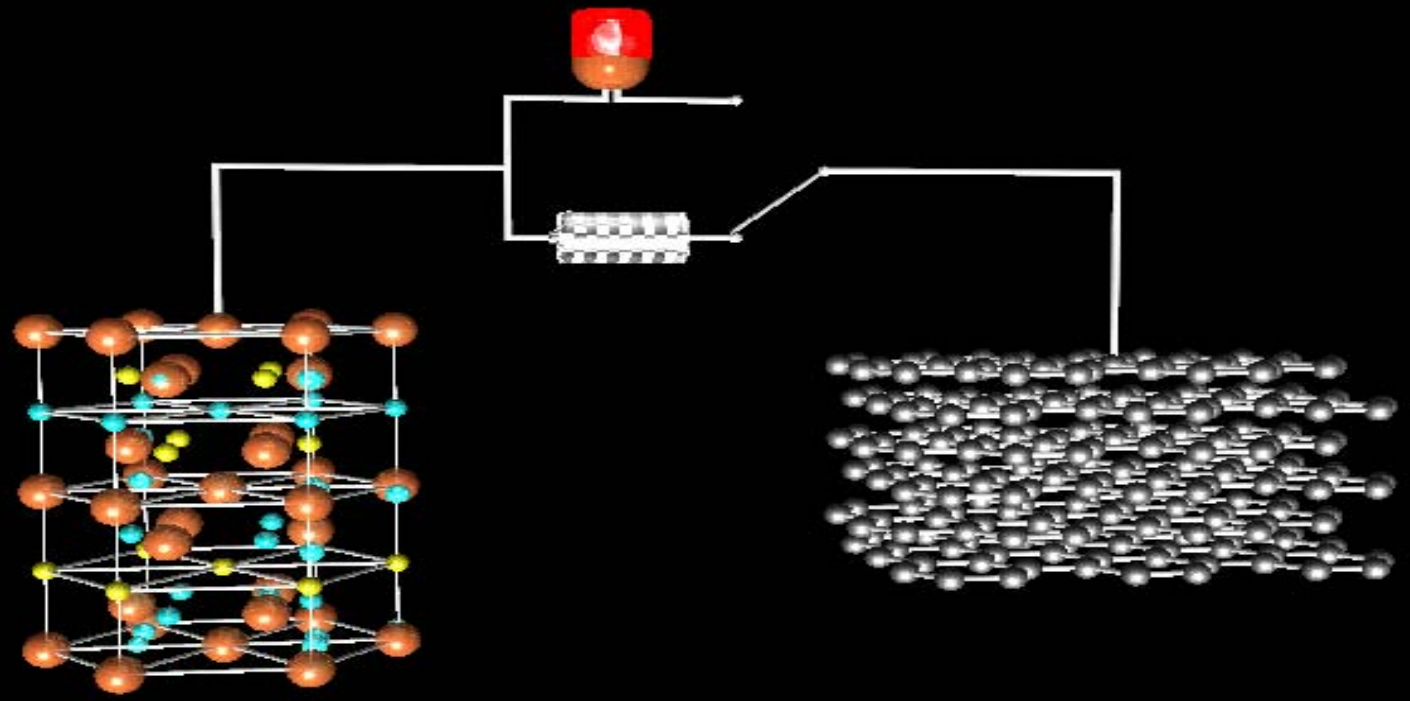

- Li
- O
- Co

$LiCoO_2$

Graphite

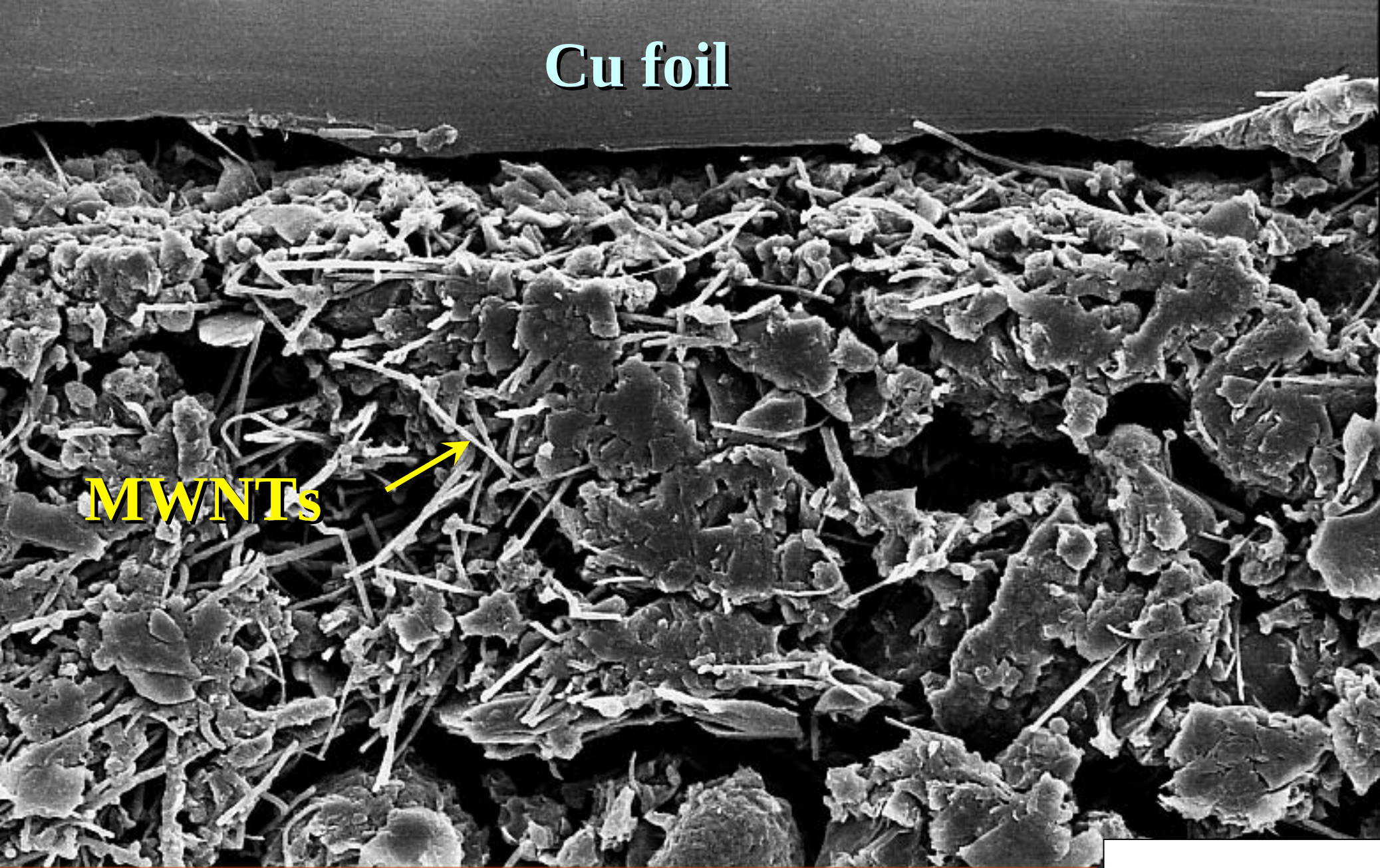

M.Endo, Y.A.Kim, T.Hayashi, K.Nishimura, T.Matsushita, K.Miyashita and M.S.Dresselhaus; Carbon, Vol.39, pp1287-1297, (2001).

Cyclic characteristics of synthetic graphite anode as a function of weight percent of MWNTs

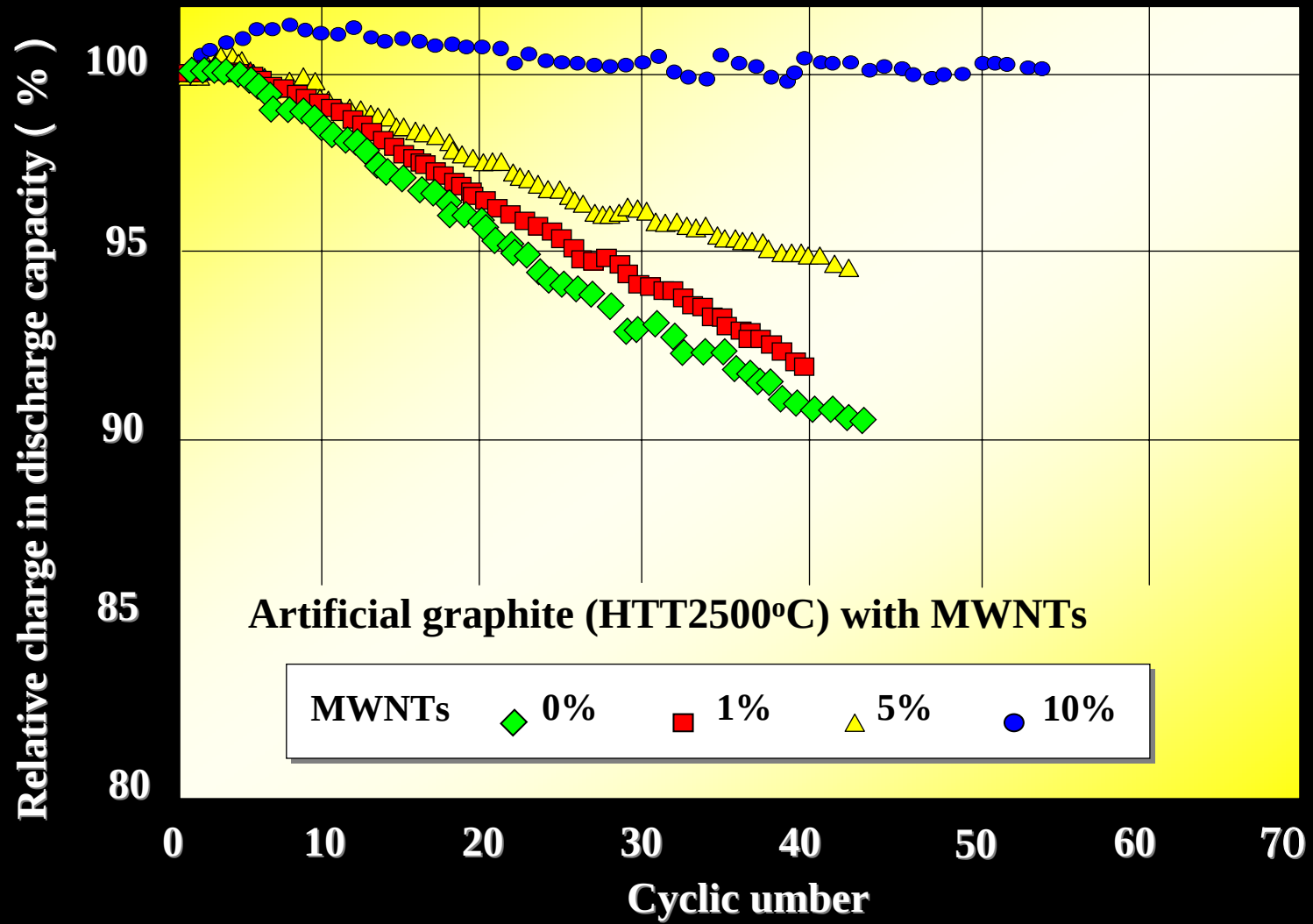

M. Endo, Y. A. Kim, T. Hayashi, K. Nishimura, T. Matsushita, K. Miyashita and M. S. Dresselhaus, Carbon, 39, 1287-1297 (2001).

Superelasticitiy of carbon nanotube; Effect of nanosize

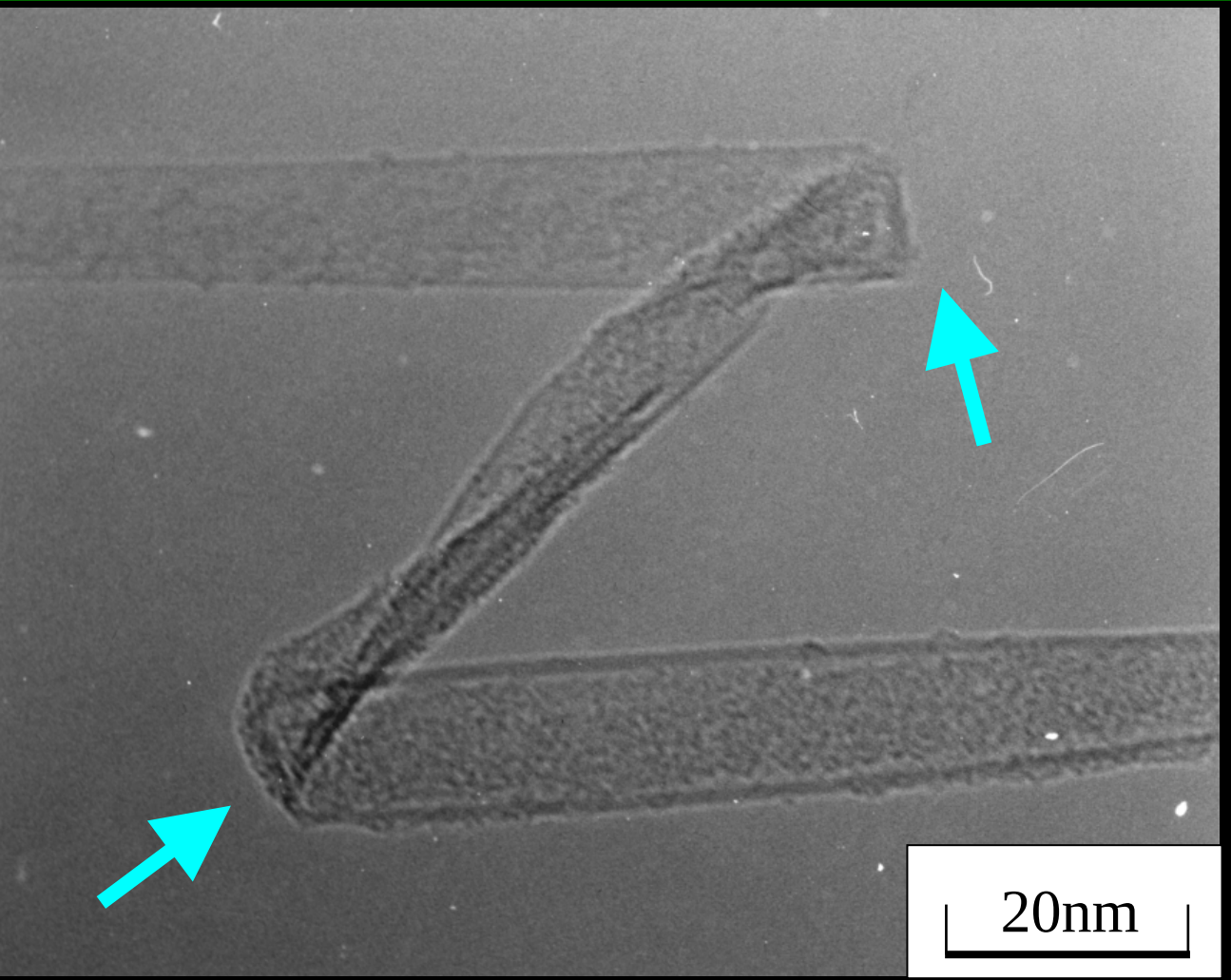

M. Endo, K. Takeuchi, K. Kobori, K. Takahashi, H. W .Kroto and A. Sarkar, Carbon, 33, 873-881 (1995).

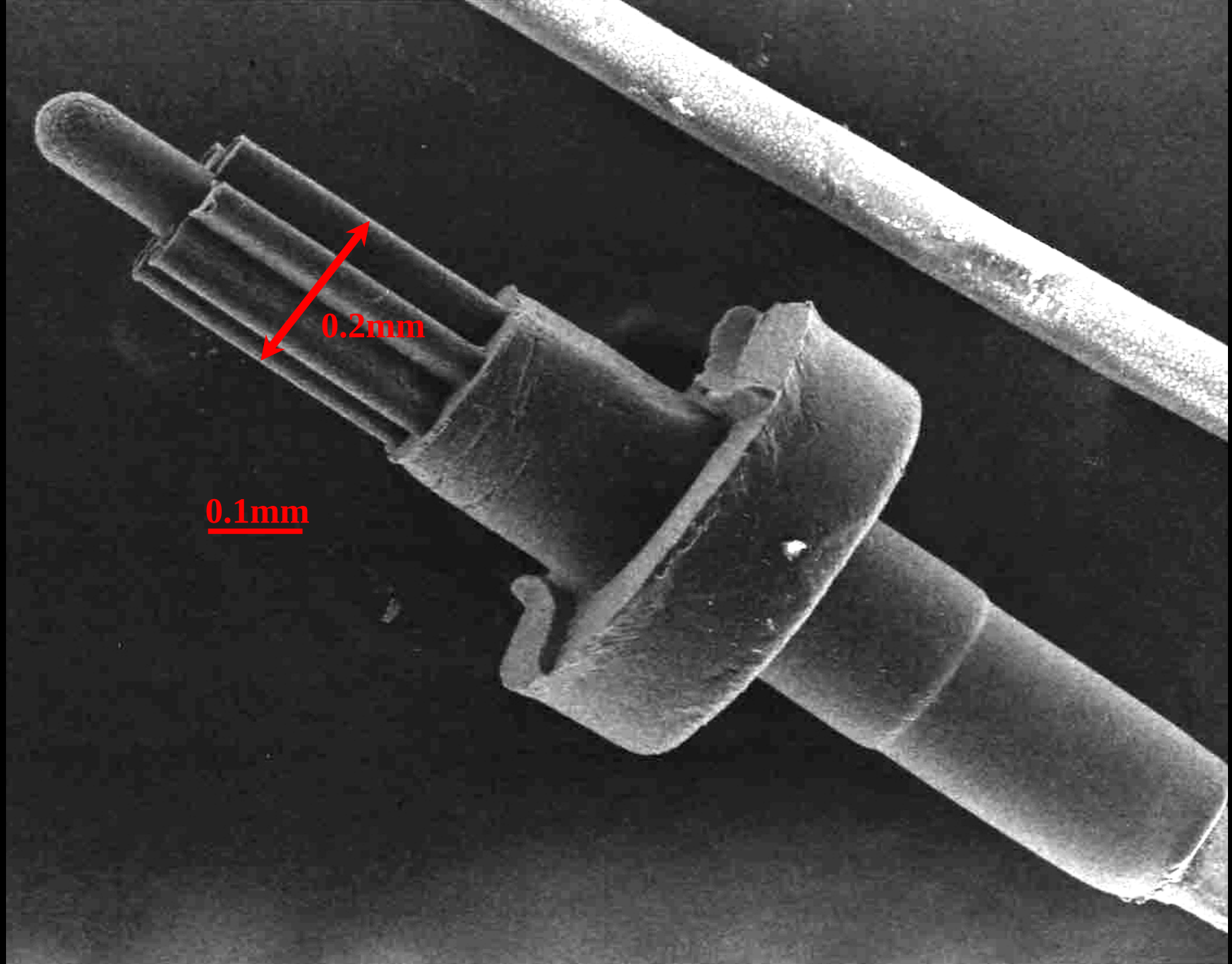
0.2mm
0.1mm

MP-001

あのMPに、ドライバーデビュー。

By
M.End

最適重心設計によるMP-001専用シャフト。

■ツアースピリットMP（400）

Buttスティッフによる弾きのよさ、高弾性カーボンファイバーによるロートルク。さらに、補強層に衝撃強度に優れたカーボンナノチューブ採用で、軽量ながらカウンターバランス設計を実現することでヘッドが利くシャフトとして完成しました。

■MP シャフト硬さ分布

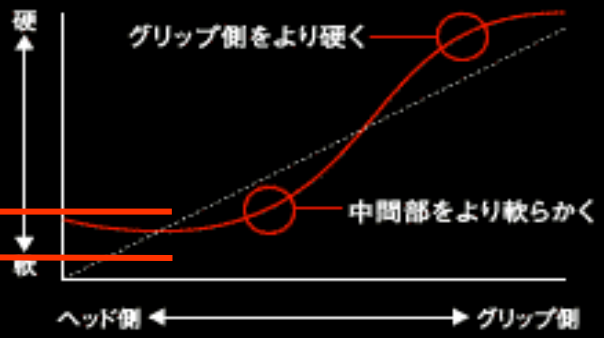

http://www.golfersland.net/mp001/lineup/f_mp001.html

Super tweeter of Carbon ＮＴ / Ｃ composite

~Realize the feeling of live atmosphere~

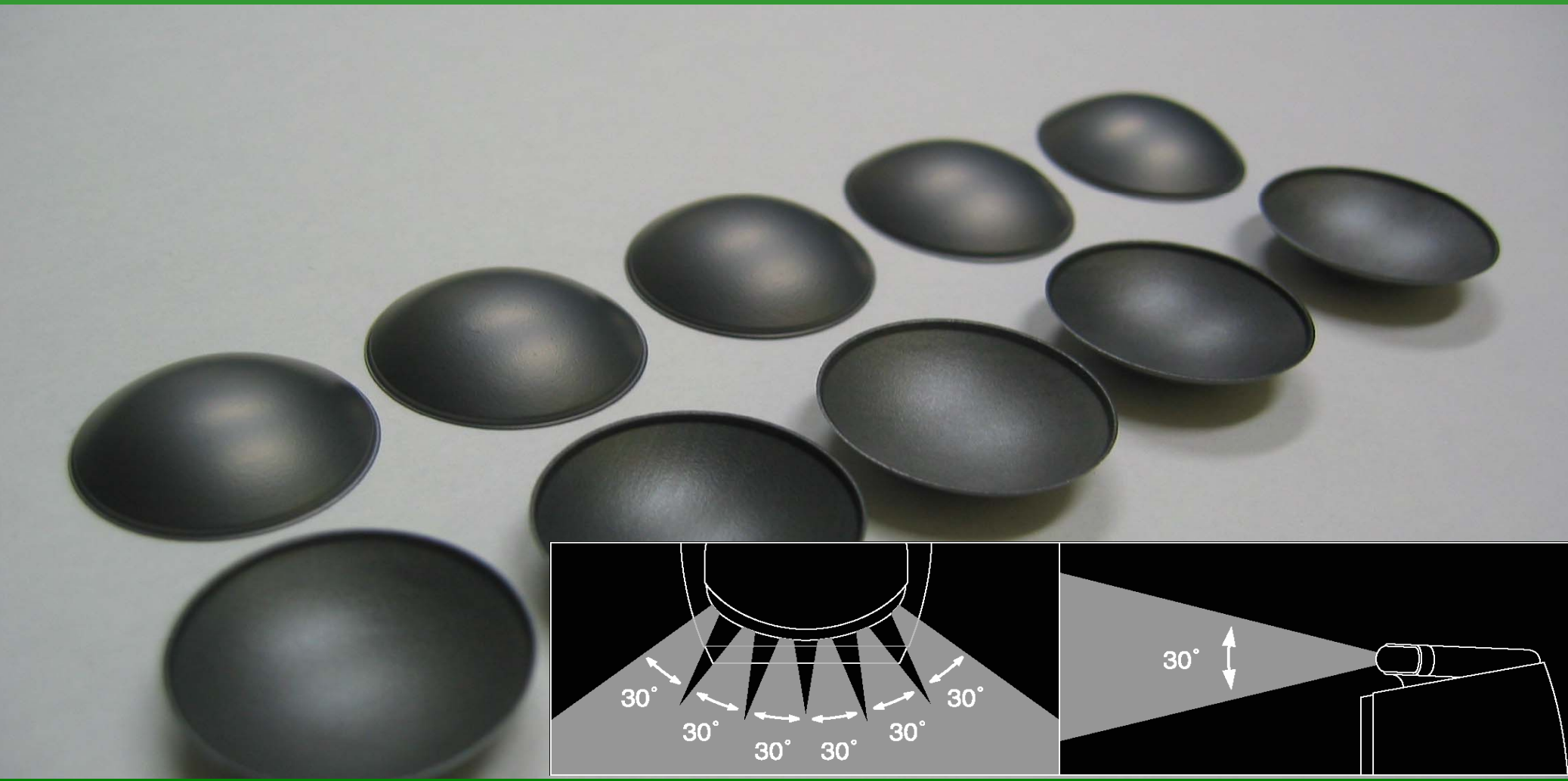

GSI Creos co ltd, Mitubishi pencil co. ltd, M. Endo

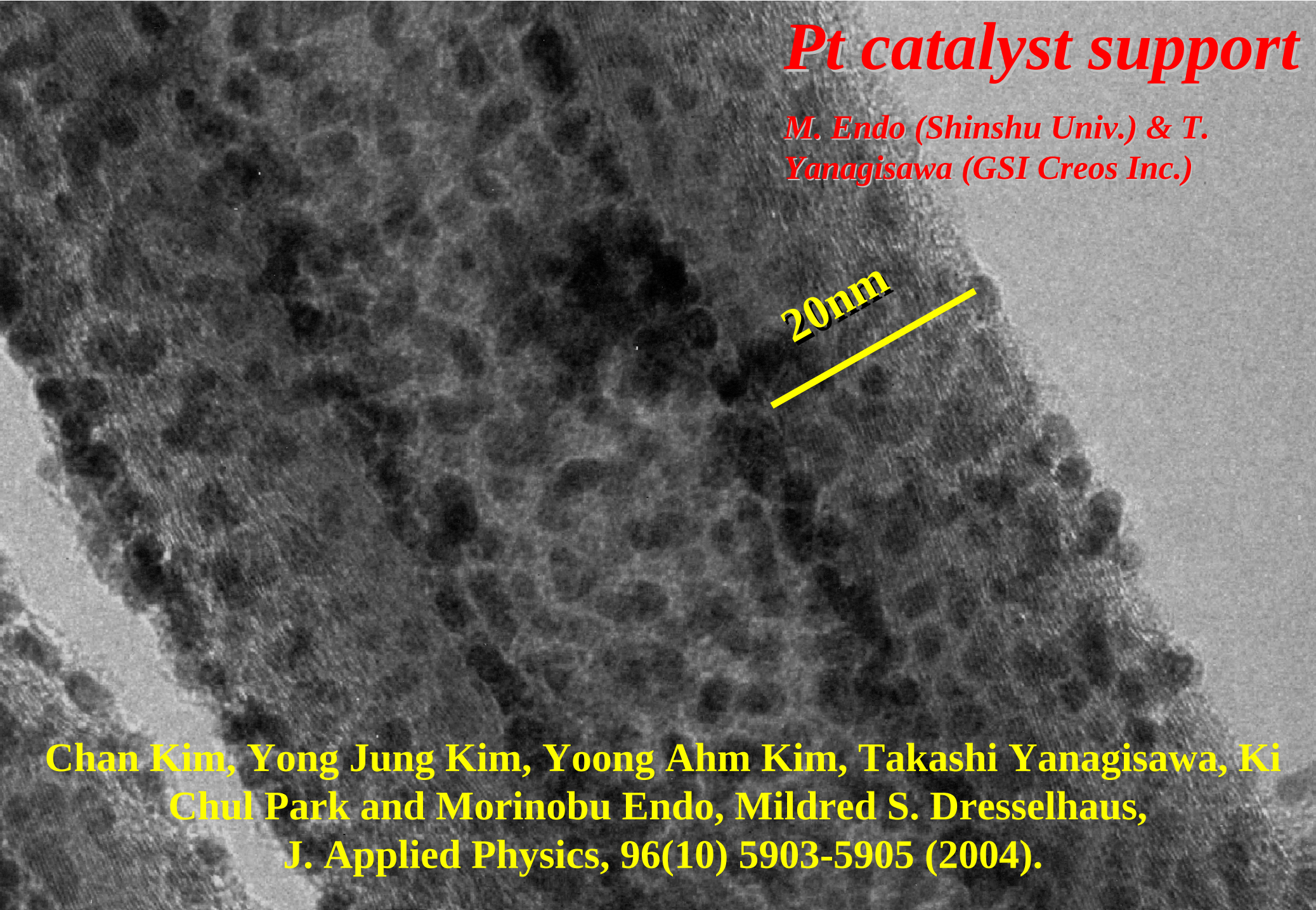

Chan Kim, Yong Jung Kim, Yoong Ahm Kim, Takashi Yanagisawa, Ki Chul Park and Morinobu Endo, Mildred S. Dresselhaus, J. Applied Physics, 96(10) 5903-5905 (2004).

Histopathological Aspects after Subcutaneous Implantation of Various Carbon Nanotubes in Mice

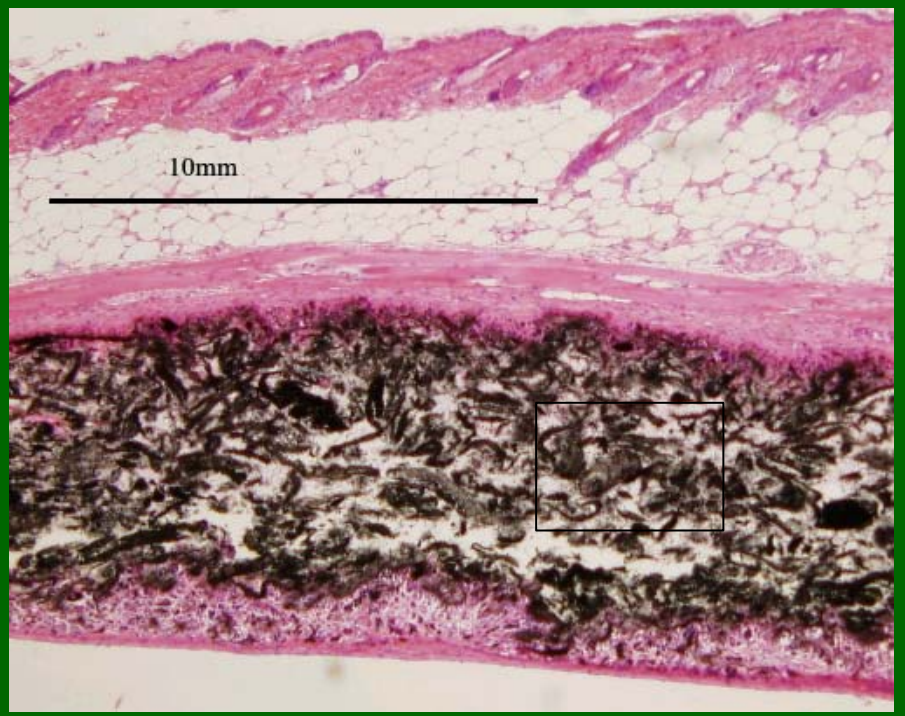

MWCNT、 4 weeks after Implantation

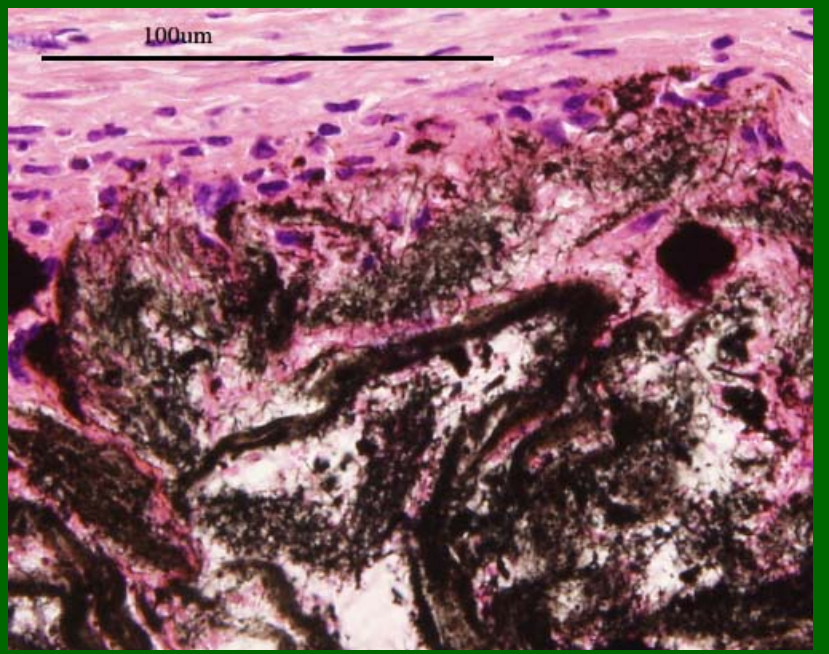

This tube induced cell infiltration without an edemoutous aspect at 1 week post-implantation. A granulomatous tissue becomes compact and tight between agglomerates of nanotubes with time.
Finally, several particles were phagocytozed over 3 weeks post-implantation. (Submitted to Carbon)

M. Endo et al., Thrombogenicity and Blood Coagulation of a Micro-Catheter Prepared from Carbon Nanotube-Nylon Based Composite
Nano Letters, 5(1), 101-106 (2005)

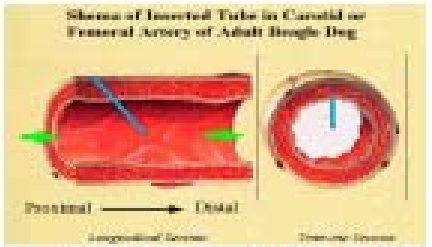

White Tube vs Black Tube

Thrombus demonstrates Dark Blue stained by HE.

Tube position shows opaque circle.

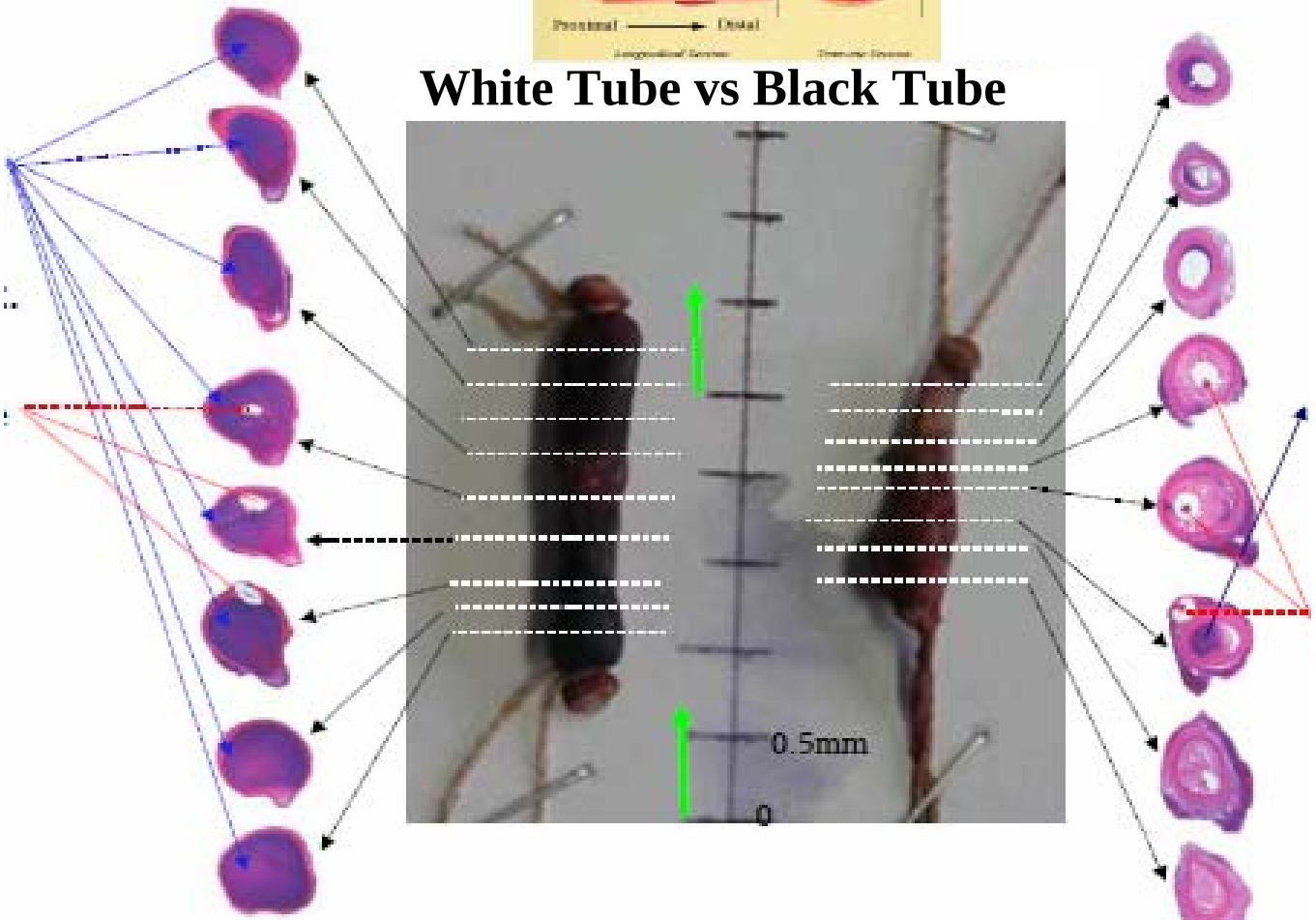

Thrombus demonstrates Dark Blue stained by HE.

Tube position shows opaque circle.

濃紫色は血栓　白では著明に形成されている。この実験は生きた犬に上段の模式図のようにチューブを留置して1 時間

M. Endo et al., Thrombogenicity and Blood Coagulation of a Micro-Catheter Prepared from Carbon Nanotube-Nylon Based Composite
Nano Letters, 5(1), 101-106 (2005).

Selective formation by Catalytic CVD Method

Possibility and Potential for Controllability of MW- ,DW- and SW-NT Structure

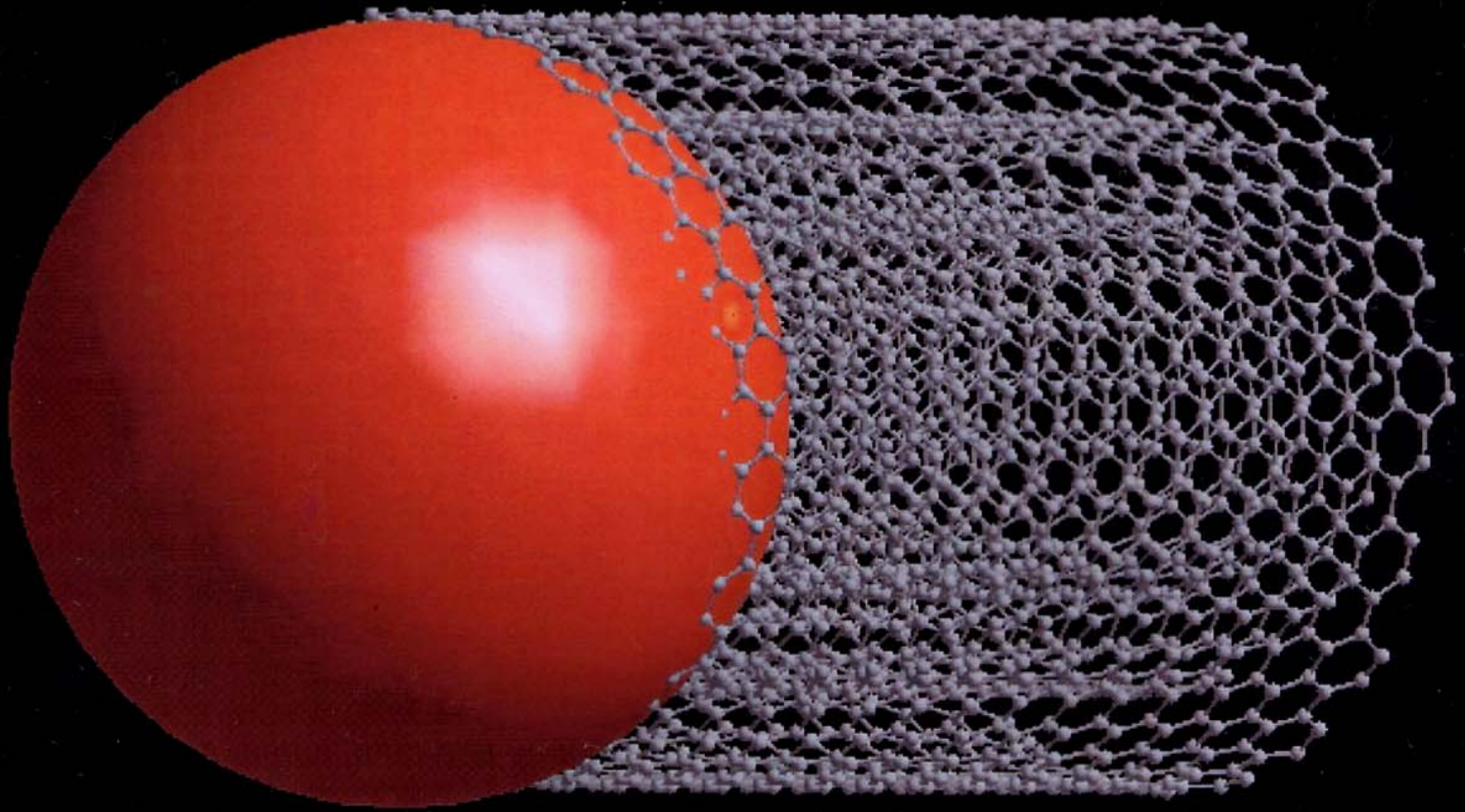

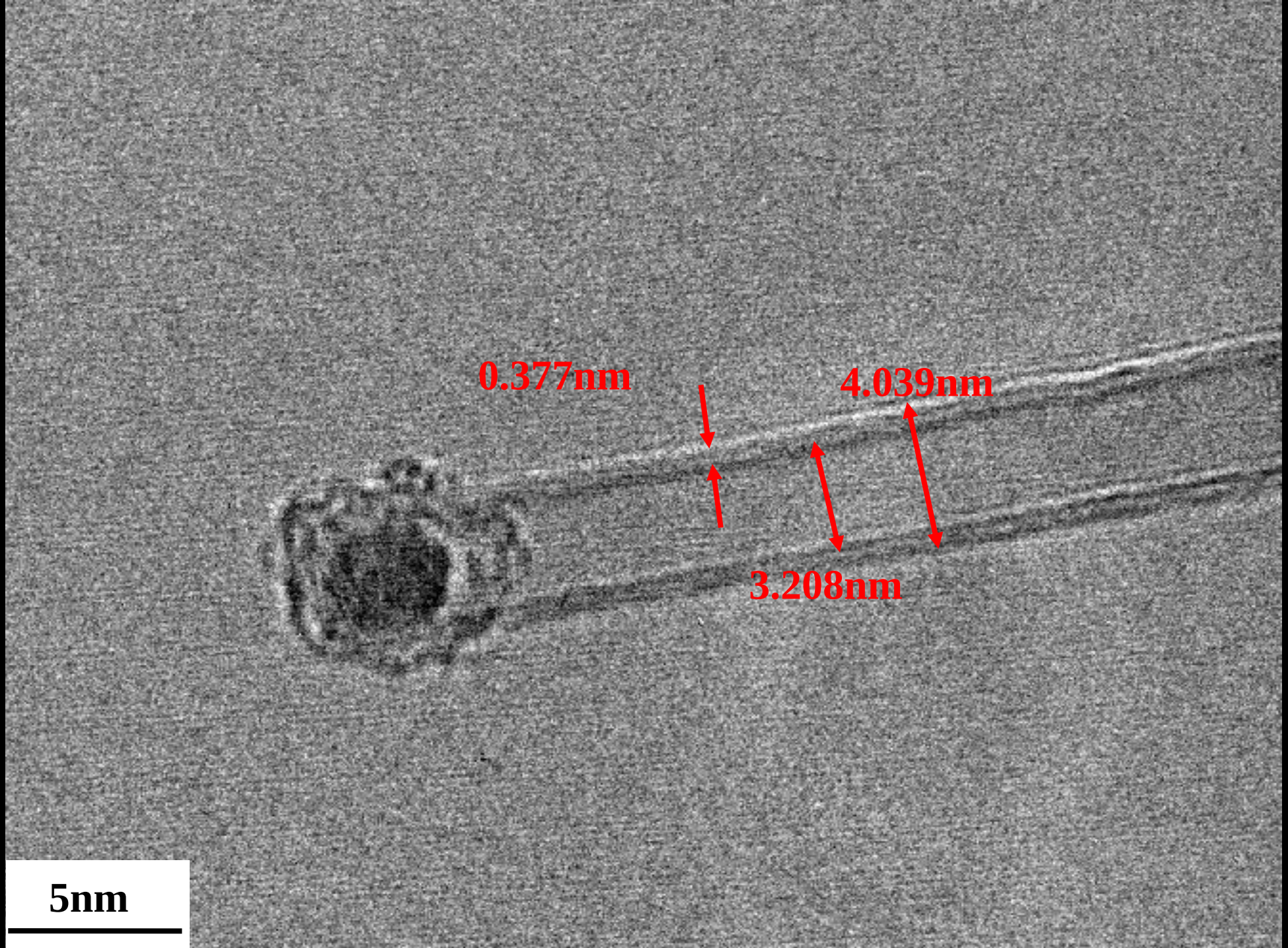
0.377nm
4.039nm
3.208nm
5nm

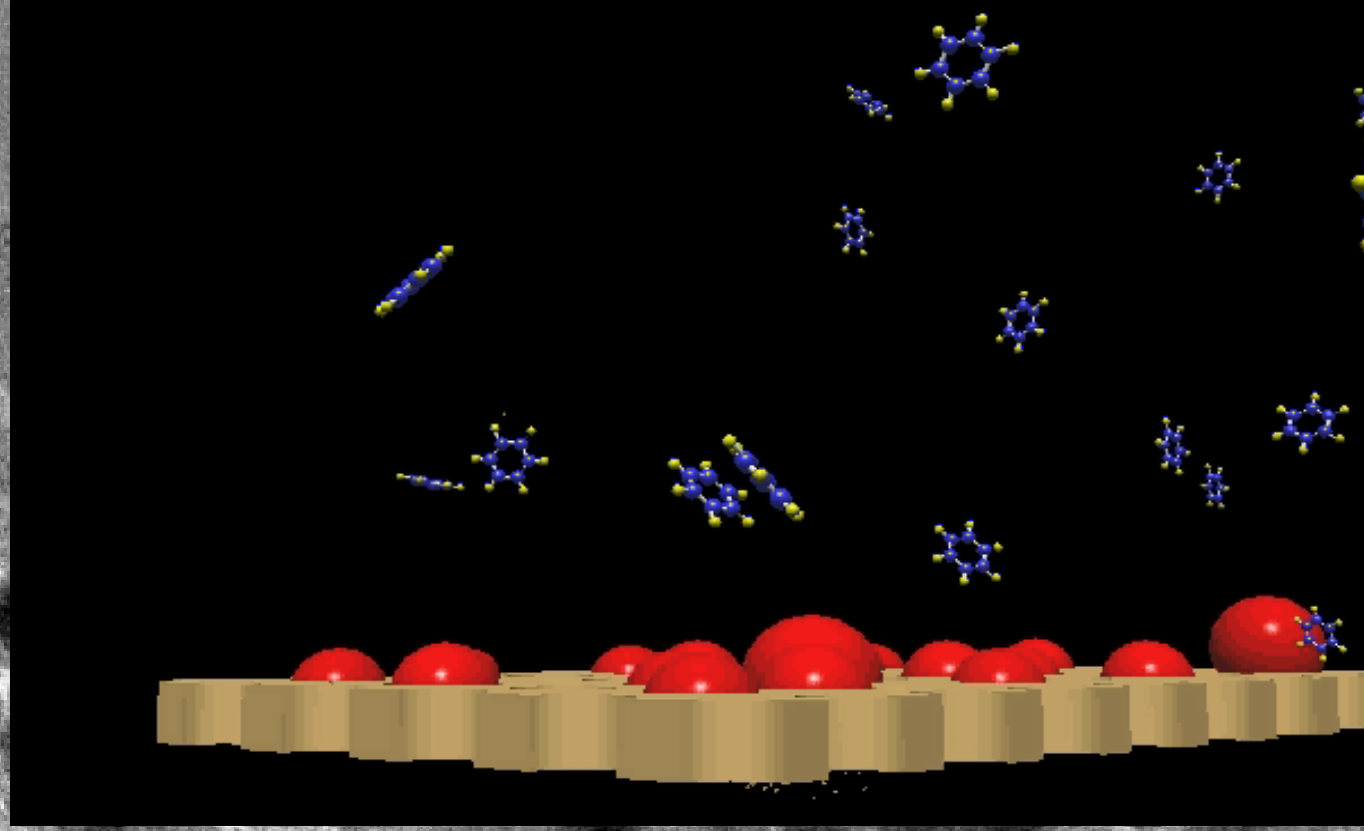

The top- or root growth of SWNT depend on the electronic interaction between metal catalyst particles and their supported substrate;

Bottom-growth; strong correlatio

Tip-growth; week correlatio

50 nm

Catalyst supported on the substrate particle

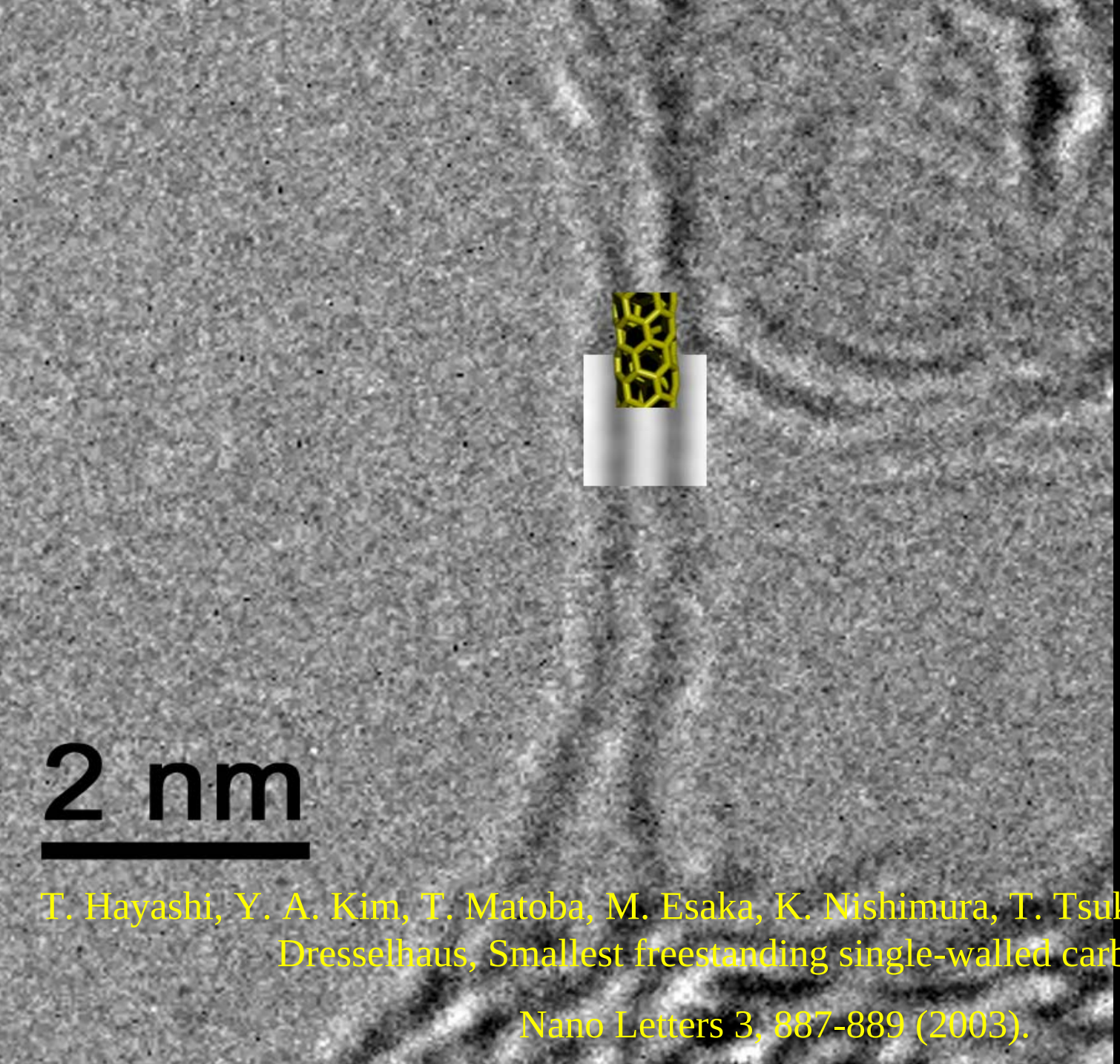

High-resolution transmission electron microscope image of a small SWNT. Inserted images are the model of (5,1) tube and the TEM simulated image, which is in good agreement with the observation.

T. Hayashi, Y. A. Kim, T. Matoba, M. Esaka, K. Nishimura, T. Tsukada, M. Endo and M.S. Dresselhaus, Smallest freestanding single-walled carbon nanotube,

Nano Letters 3, 887-889 (2003).

Highly-purified DWNT sheet

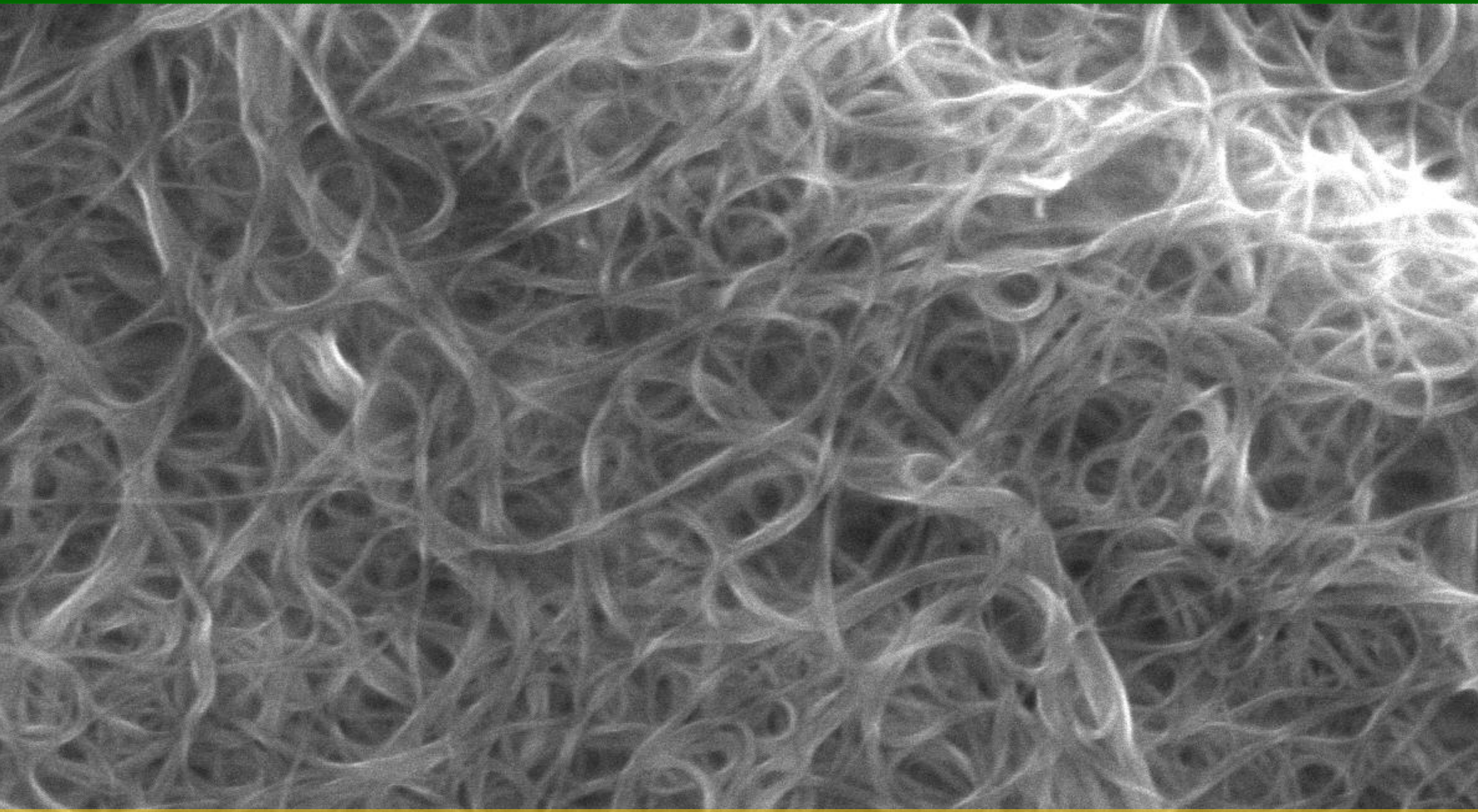

M. Endo, H. Muramatsu, T. Hayashi and Y. A. Kim, M. Terrones, M. S. Dresselhaus, Nature 433, 476 (2005).

High purity DWNTs by CCVD Method, by M. Endo et al., Nature 433, 476 (2005).

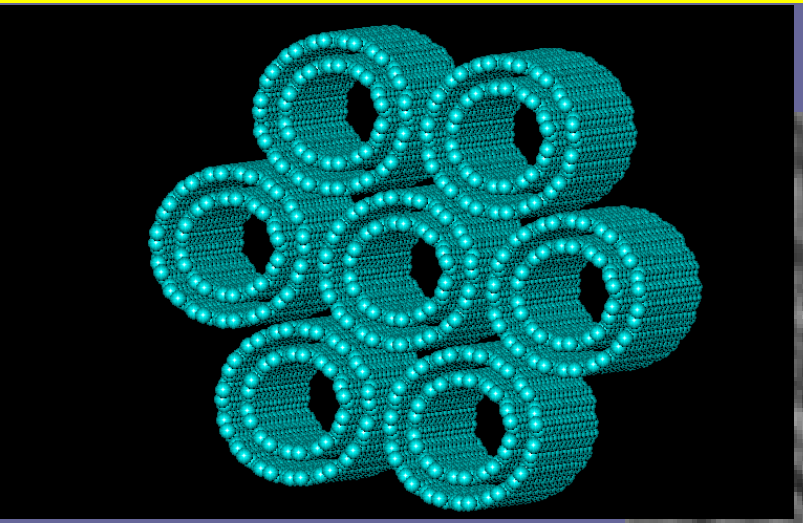

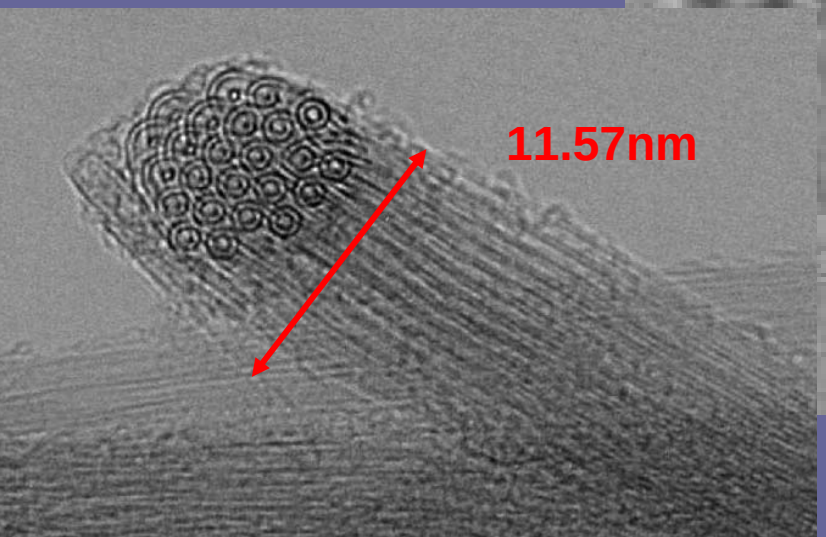

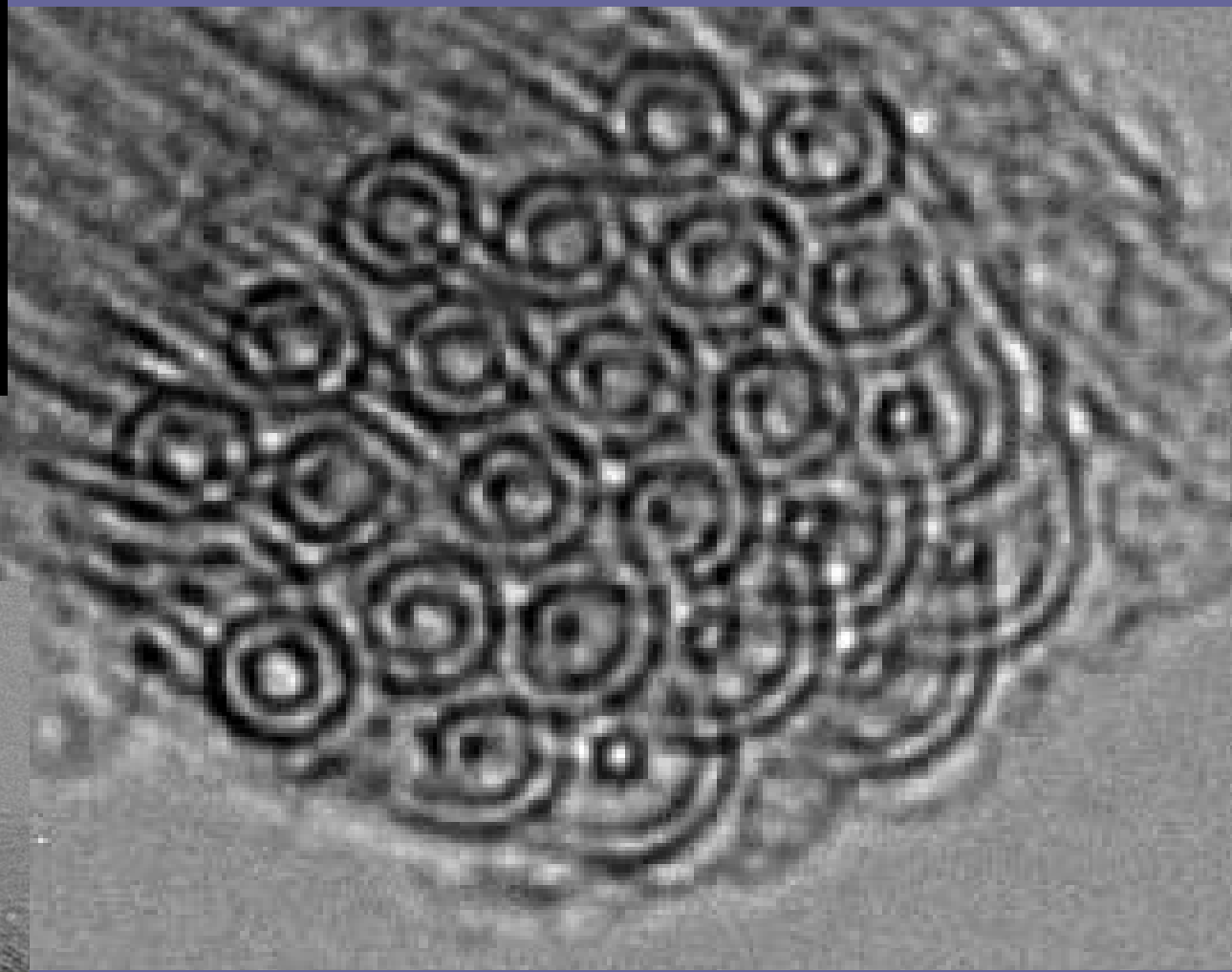

Raman Scattering of B-doped DWNTs

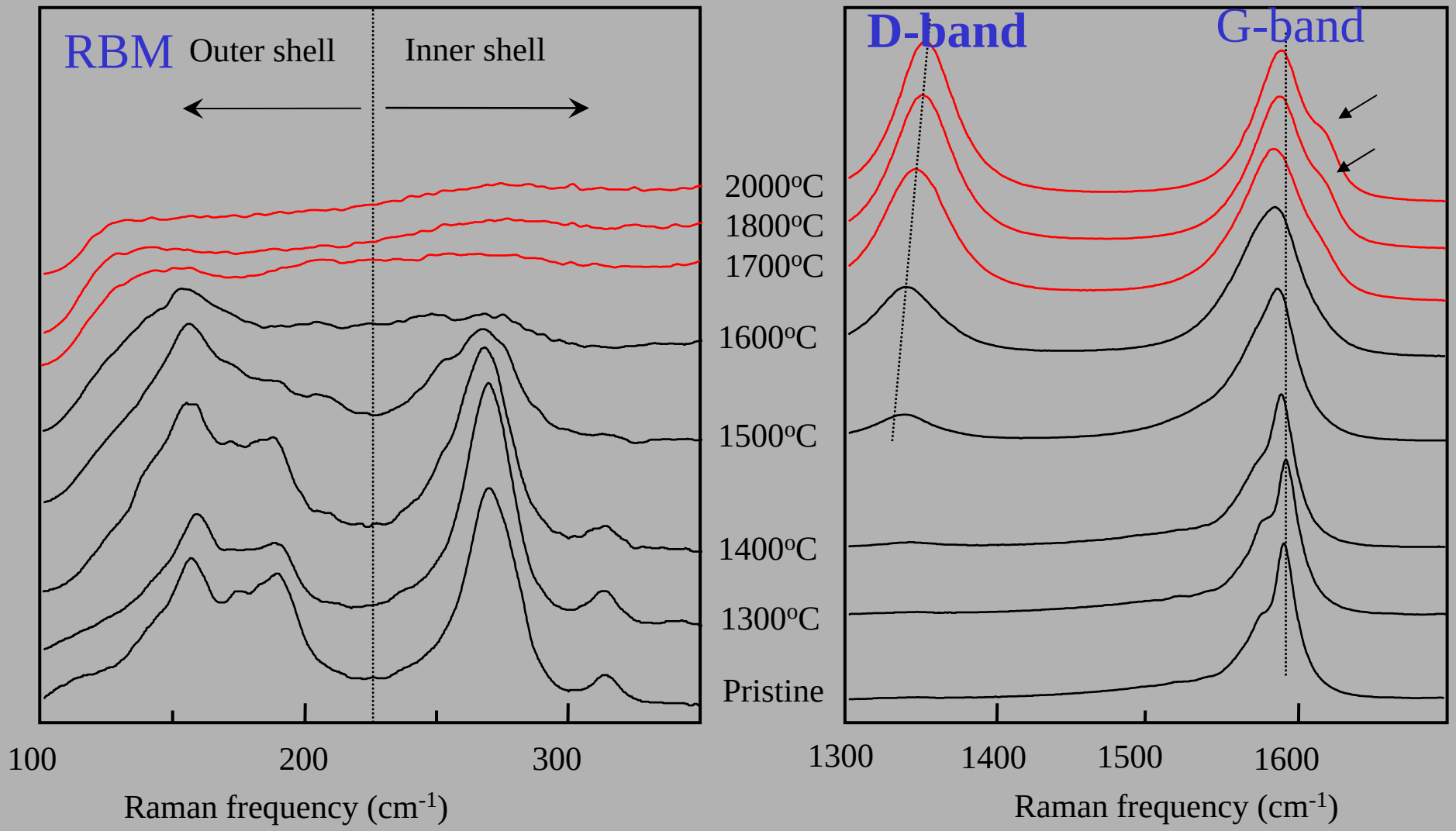

The disappearance of the RBM frequency is a direct indicator of the destruction of the original DWNTs and of diameter-enlarged DWNTs, MWNTs and graphitic material as the final formation by thermal treatment.

HR-TEM images of B-doped DWNTs

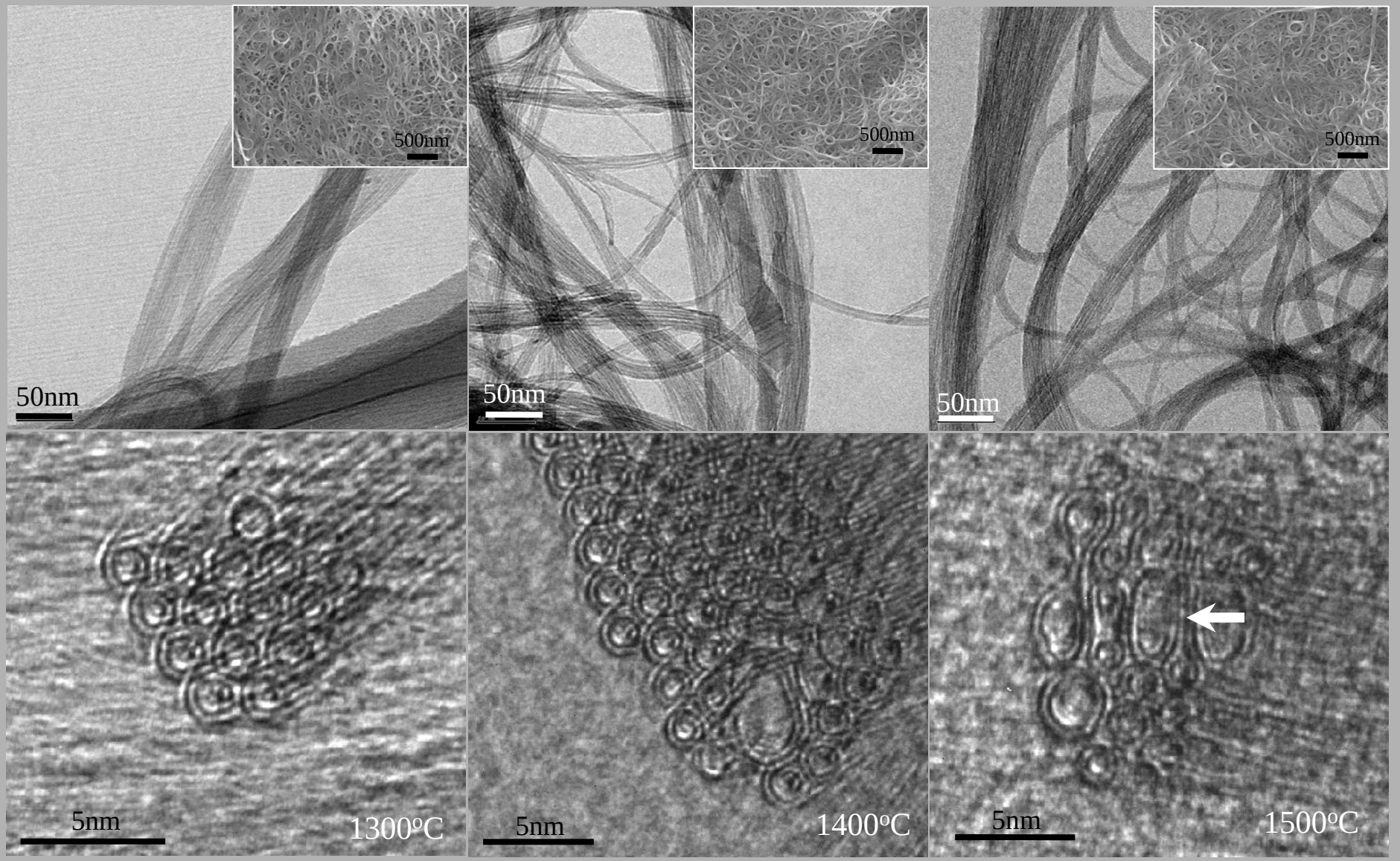

Miracles of Nano

Comparison of running speed and body length

6 times

10 times

20 times

(10mm/min,83μm/s)

8,000 times of catalytic particle size

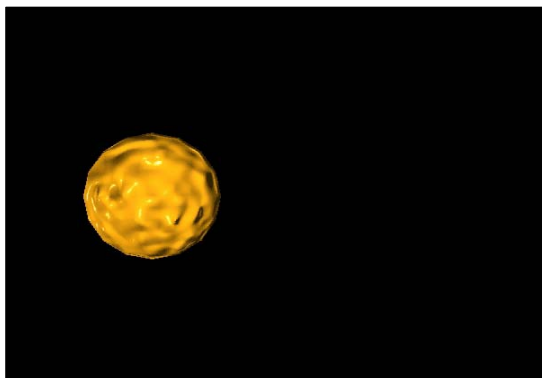

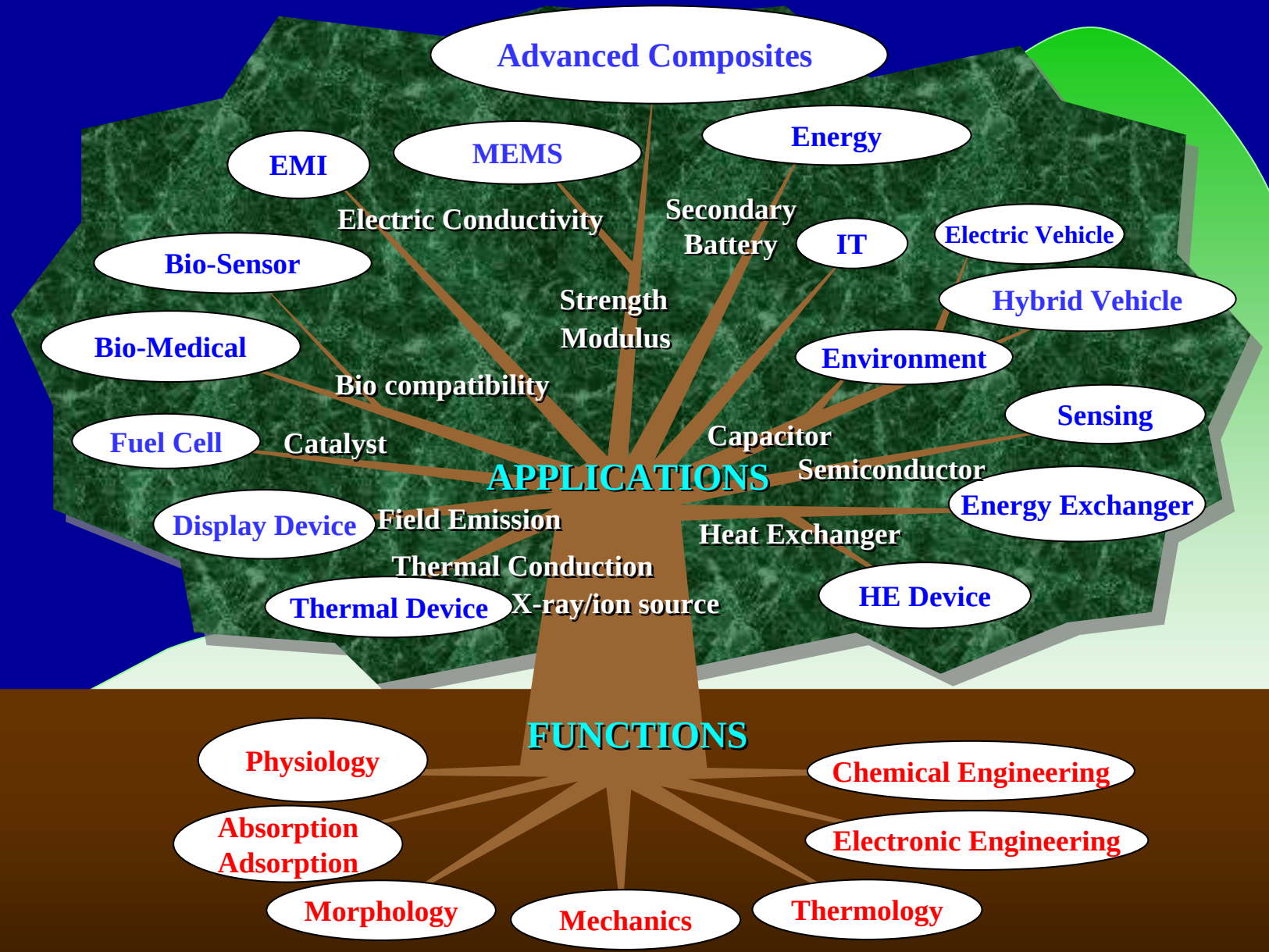

Functions and Applications of Carbon NTs

M.Endo

CONCLUSIONS

1. **Large-scale production of carbon nanotubes by a catalytic chemical vapor deposition (CVD) method has been widespread in a worldwide level, and their practical applications are going to expand in a wide range of fields.**

2. **With respect to scientific and engineering issue, new breakthroughs including more effective and controllable synthesis of carbon nanotubes are critically required when considering wide range of huge markets in the range from energy device, composite to electronic device. Giga-level of nanomaterials-based market will be opened in the near future.**